Robust thermal stability for batch process intensification with model predictive control

A. Kanavalau, R. Masters, W. Kähm*, V. S. Vassiliadis

Department of Chemical Engineering and Biotechnology, West Cambridge Site, Philippa Fawcett Drive, University of Cambridge, Cambridgeshire, CB3 0AS, United Kingdom

Abstract

Thermal runaways in exothermic batch reactors present major safety and economic issues for industry. Control systems currently used are not capable of detecting thermal runaway behaviour and achieve nominally safe operation by carrying out the reaction at a low temperature. Recently, improvements in safety and process intensity have been achieved by using Model Predictive Control (MPC) with embedded stability criteria. The reliance of this approach on accurate model predictions makes plant-model mismatch a crucial issue. The most common source of plant-model mismatch is uncertainty of model parameters. Scenario-based MPC and worst case MPC are used with stability criterion $\mathcal{K}$ and Lyapunov exponents in this work. The effect of all uncertain parameters on thermal runaway potential can be identified easily for simulations in this work. Hence, worst case MPC results in a computationally more efficient control scheme than scenario-based MPC, whilst ensuring the same extent of safety and process intensification.

Keywords: thermal stability, robust control, model predictive control, process intensification

1. Introduction

Batch processes account for a large fraction of industry due to the flexible nature of such processes. Many batch processes are exothermic in nature and hence generate heat during the reaction. If more heat is generated than can be removed, the temperature and pressure increase uncontrollably resulting in thermal runaway behaviour. This potentially causes the release of hazardous chemicals into the environment as well as unsafe working conditions in the plant (Theis, 2014). Furthermore, interruptions in normal operation due to thermal runaways also have detrimental effects on the ecology of industrial plants. Identifying when thermal runaways occur hence presents an important task for industry in order to avoid such events.

*Corresponding author
Email address: `wk263@cam.ac.uk` (W. Kähm)

Most batch processes in industry are run at a constant temperature with Proportional-Integral-Differential (PID) control (Winde, 2009; Stephanopoulos, 1984) to avoid thermal runaways. The reactor temperature can be increased during the process in a safe manner, if the system stability is known. This potentially reduces the reaction time significantly, making the batch processes safer and more efficient. In this work the term "batch intensification" hence refers to the reduction in batch duration obtained by an increase in reaction temperature throughout the process.

For continuous stirred tank reactors (CSTRs) stability criteria found in literature work well, *e.g.* the theory of heat explosion (Semënov, 1940), the Barkelew criterion (Barkelew, 1959), the Balakotaiah criterion (Balakotaiah, 1989), the Baerns criterion (Baerns and Renken, 2004), the Frank Kaminet͡skiĩ criterion (Frank-Kamenet͡skiĩ, 1969), and the Routh-Hurwitz criterion (Anagnost and Desoer, 1991; Stephanopoulos, 1984; Hurwitz, 1895; Routh, 1877). All of the above criteria, except the Routh-Hurwitz criterion, are based on the Semënov theory of heat explosions (Rupp, 2015). Hence, if the Semënov criterion predicts the thermal stability of batch processes unreliably, the Barkelew, Balakotaiah, Baerns and Frank-Kaminet͡skiĩ criterion are not appropriate for such systems, either.

Stability criteria based on Lyapunov functions were implemented in systems operating at steady state. A good review for such systems is given by Albalawi et al. (2018). Good results were obtained for continuous industrial systems, which have a clearly defined steady state, with such an approach (Zhang et al., 2018; Albalawi et al., 2017, 2016). Since batch reactors are inherently non-steady state, this approach cannot be extended to such systems easily.

For batch reactors other stability criteria for predicting thermal runaway behaviour exist, one of which is the divergence criterion (Bosch et al., 2004; Strozzi and Zaldívar, 1999). In Kähm and Vassiliadis (2018d) it was shown that for some batch processes the divergence criterion systematically over-predicts the system instability. Hence it cannot be used to intensify such batch processes. Thermal stability criterion $\mathcal{K}$ (Kähm and Vassiliadis, 2018c,d) and Lyapunov exponents (Kähm and Vassiliadis, 2018a,b) are shown to work reliably for batch processes. Thermal stability criterion $\mathcal{K}$ results in less computational time than Lyapunov exponents. Furthermore, Lyapunov exponents require careful tuning to make them reliable for batch processes (Kähm and Vassiliadis, 2018b).

With Model Predictive Control (MPC) it is possible to incorporate stability detection within a control framework. MPC continuously evaluates the reactor temperature set-point whilst taking into account system constraints, including the system stability (Chuong La et al., 2017; Anucha et al., 2015; Mayne, 2014; Christofides et al., 2011). PID control cannot take such constraints into account (Winde, 2009; Stephanopoulos, 1984). A fundamental requirement for the application of MPC to industrial systems is the reliable and quick detection of stability during the process and evaluation of control actions to be applied.

MPC requires the use of a process model, according to which the optimal sequence of control inputs are evaluated. In industry it is rarely possible to find process models which are 100% accurate for such purposes. Parameters within the model can be uncertain (Kalmuk et al., 2017; Sirohi and Choi, 1996) or the model might have the wrong structure, often called model-plant mismatch (Hong et al., 2012; Badwe et al., 2010). Uncertainty in the process model can have significant effects on process control if not taken into account. The ability to keep a process under control whilst experiencing uncertainties is called *robust control*.

The structure of models for chemical reactor systems can often be found from first principle techniques. The biggest issue becomes the estimation of the parameters within the model (Dochain, 2003). From plant measurements the parameters can be estimated, but uncertainty will still be present.

For chemical reactor systems the effect of each parameter can often be identified, *e.g.* an increase in enthalpy of reaction ΔH_r will increase the amount of heat released. This property enables the identification of the *worst* set of parameters for the system model, *i.e.* the set of parameters that makes the process as unstable as possible. This idea led to the development of the open-loop min-max MPC approach (Campo and Morari, 1987). This approach assumes the most unstable set of parameters for which a stable system is obtained. If the most unstable process can be kept under control, the real process will be kept stable as well. This results in overly conservative control since feedback of the MPC throughout the process is not taken into account (Martí et al., 2015; Lucia et al., 2014).

One approach to deal with uncertainty is the continuous estimation of the process model with the use of Gaussian processes (Kocijan et al., 2004; Jones et al., 1998). This method uses the maximum likelihood estimator of the process model with samples from the process to find the most likely model. Several case studies in literature were considered using this approach (Bradford et al., 2018; Maciejowski and Yang, 2013; Likar and Kocijan, 2007). Other approaches to overcome the limitation of the open-loop control are closed-loop min-max MPC (Rakovic et al., 2011; Rawlings and Animit, 2009; Mayne et al., 2005) and tube-based MPC (Muñoz-Carpintero et al., 2016). These methods take into account that new information will be available as the process occurs, but issues with respect to overly conservative control and computational cost arise.

To avoid the overly conservative nature of closed-loop min-max MPC, a multistage MPC framework was developed (Martí et al., 2015; Lucia et al., 2013; Bernadini and Bemporad, 2009; Scokaert and Mayne, 1998). This method assumes that the uncertainty within the system can be represented by multiple scenarios with state variables x, each representing a possible set of parameters in the model. For parametric uncertainty only one stage is required, because a value for each uncertain parameter can be sampled independently. Each set of parameter values can then be used as a single scenario. This work addresses the issue of parametric uncertainty on the $\mathcal{K}$ stability criterion, as well as Lyapunov exponents.

When using thermal stability criteria with MPC this implies that the effect of uncertainty on these stability measures has to be identified in detail. Once it is observed how each stability criterion behaves under model-plant mismatch, an MPC framework incorporating thermal stability criteria can be used.

This work focuses on achieving the following goals:

- verify the validity of the Semënov and Routh-Hurwitz criterion for batch processes
- examine the effect of uncertainty on reliable stability measures
- develop a robust MPC framework using suitable thermal stability criteria
- intensify batch processes safely with the proposed control framework

Achieving these goals results in a novel approach to reduce the reaction time for batch processes in a safe manner, whilst considering parametric uncertainty.

This paper is organised as follows: in Section 2 the batch reactor model used for all simulations is presented. The Semënov and Routh-Hurwitz criteria are examined in Section 3. In Section 4 the robustness of thermal stability criterion $\mathcal{K}$ and Lyapunov exponents are examined. A robust MPC scheme incorporating these stability criteria is presented and examined in Section 5. The key results and future work required are summarised in Section 6.

2. Batch reactor model

To carry out dynamic simulations of batch reactors in this work, all mass and energy balances with all process parameters are necessary. These equations and parameter values are presented in the following sections.

2.1. Mass and energy balances

To model the processes occurring within a batch reactor, all relevant mass and energy balances have to be formulated. The following irreversible exothermic chemical reaction is considered in this work:

$$\mathrm{A} + \mathrm{B} \rightarrow \mathrm{C} \tag{1}$$

The rate of reaction corresponding to Equation (1) is given by an Arrhenius expression (Davis and Davis, 2003):

$$r = k_0 \, \exp\left(\frac{-E_a}{R\,T_\mathrm{R}}\right) \, [\mathrm{A}]^{n_\mathrm{A}} \, [\mathrm{B}]^{n_\mathrm{B}} \tag{2}$$

where r is the rate of reaction, k_0 is the Arrhenius pre-exponential factor, E_a is the activation energy, R is the universal molar gas constant, T_R is the reactor temperature, [A] and [B] are the concentrations of reagents A and B, respectively, and n_A and n_B are the orders of reaction with respect to A and B, respectively.

Using the reaction kinetics the mass balances for components A, B and C can be found:

$$\frac{\mathrm{d}\,[\mathrm{A}]}{\mathrm{d}t} = -r \tag{3a}$$

$$\frac{\mathrm{d}\,[\mathrm{B}]}{\mathrm{d}t} = -r \tag{3b}$$

$$\frac{\mathrm{d}\,[\mathrm{C}]}{\mathrm{d}t} = +r \tag{3c}$$

where r is given by Equation (2) and t is the time of simulation.

Since an exothermic reaction is present, heat is generated during the batch process. The generation of heat will cause a change in temperature, determined by the relevant energy balances. The energy balance of the reactor contents is given by:

$$\frac{\mathrm{d}}{\mathrm{d}t}\left(V_\mathrm{R}\,\rho_\mathrm{R}\,C_{p,\mathrm{R}}\,T_\mathrm{R}\right) = r\left(-\Delta H_r\right)V_\mathrm{R} - U\,A\,\left(T_\mathrm{R} - T_\mathrm{C}\right) \tag{4}$$

where V_R is the reactor volume, ρ_R is the density of the reactor contents, $C_{p,\mathrm{R}}$ is the heat capacity of the reactor contents, ΔH_r is the enthalpy of reaction, U is the heat transfer coefficient between the coolant and the reactor contents, A is the heat transfer area between the cooling jacket and the reactor, and T_C is the coolant temperature.

A stirrer is present in the batch reactor, but its contribution to the total heat generation is negligible in comparison to the heat generated by the exothermic reaction.

Since cooling is applied, the temperature of the coolant is subject to change with time. The energy balance of the cooling jacket is given by:

$$\frac{\mathrm{d}}{\mathrm{d}t}\left(V_\mathrm{C}\rho_\mathrm{C}C_{p,\mathrm{C}}T_\mathrm{C}\right) = q_\mathrm{C}\rho_\mathrm{C}C_{p,\mathrm{C}}\left(T_{\mathrm{C,in}} - T_\mathrm{C}\right) + U A\left(T_\mathrm{R} - T_\mathrm{C}\right) \tag{5}$$

where V_C is the cooling jacket volume, ρ_C is the coolant density, $C_{p,\mathrm{C}}$ is the coolant heat capacity, q_C is the coolant flow rate, and $T_{\mathrm{C,in}}$ is the coolant inlet temperature. With Equations (2)$-$(5) the batch reactor dynamics can be simulated.

2.2. Batch reactor parameters

Batch reactors are a major part of the polymer and pharmaceutical industry. This is due to their flexibility in reaction conditions, enabling to achieve high yields for good quality products.

The reaction is initiated after all reagents are added. Usually the reagents are heated up after being added to a batch reactor. The time required to heat up the reagents is neglected for simplicity. Once the target conversion is achieved, the products are removed and the reactor is prepared for the next batch process. A schematic of the batch reactor model in this work is shown in Figure 1.

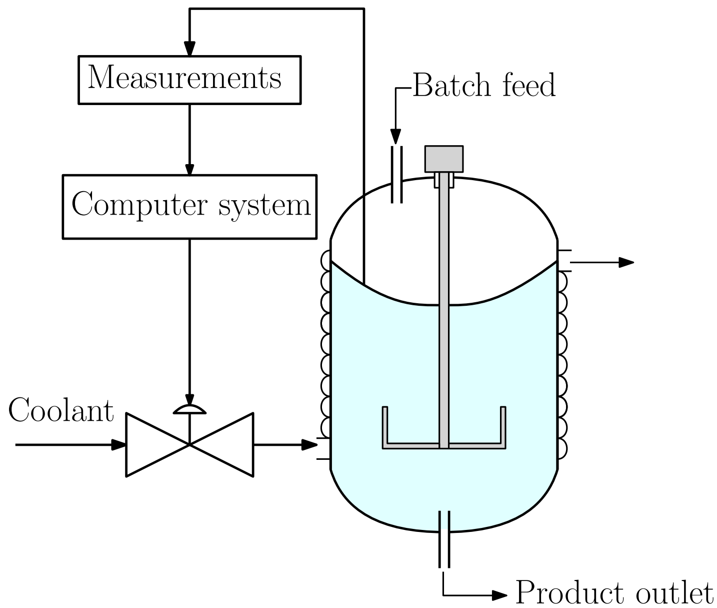

Figure 1: Batch reactor diagram for simulated systems.

In Figure 1 it is seen that a cooling jacket is present which is used to control the temperature within the reactor. This control can either be achieved by PID control (Winde, 2009; Stephanopoulos, 1984), or MPC (Chuong La et al., 2017; Rawlings and Mayne, 2015; Christofides et al., 2011). The coolant flow rate through the cooling jacket is controlled by a valve which is open if maximum cooling is required, or completely closed if no cooling is necessary. Measurements of the reactor temperature and all concentrations give feed back on how close the system is to the specified set-point. This will set the cooling valve position for both PID control and MPC.

A stirrer is also present in order to make sure good mixing is present within the reactor. Strong mixing ensures that all physical properties in the reacting mixture can be assumed to be uniform.

In industry various sizes of batch reactors exist for particular chemical reactions. A total of six reactions are considered in this work:

1. 5 example reactions according to which the reliability of stability criteria is examined, called processes $P_1 - P_5$
2. the nitration of toluene, for which the robust MPC frameworks are applied and their performance assessed

The data of the different reactor settings used for each reaction in this work are shown in Table 1.

Table 1: Batch reactor parameters for the processes considered.

Process	V_R $[m^3]$	V_C $[m^3]$	A $[m^2]$	$q_{C,max}$ $[m^3\,s^{-1}]$	U $[W\,m^{-2}\,K^{-1}]$
$P_1 - P_5$	20	1.4	36	0.030	600
Nitration of toluene	8.0	0.50	20	0.023	500

The values of V_R shown in Table 1 represent the volume of the reagents and not the volume of the whole reactor. This is the case because the stirring action and potential foam formation requires additional space within the reactor.

The data for all chemical reactions considered in this work are given in Table 2.

Table 2: Batch reactor parameters for the processes considered in this work.

Process	k_0	n_A;n_B	$\Delta H_r \times 10^{-3}$	E_a/R	[A]	[B]
	$[m^{3n-3}\,kmol^{1-n}\,s^{-1}]^*$	$[-]$	$[kJ\,kmol^{-1}]$	[K]	$[kmol\,m^{-3}]$	$[kmol\,m^{-3}]$
P_1	2.76×10^6	1;0	-75.0	9525	13	21
P_2	5.00×10^3	1.5;0	-110	9480	13	13
P_3	2.20×10^2	3;1	-250	9525	13	18
P_4	9.70×10^4	1.5;1	-130	9550	8.0	12
P_5	3.00×10^5	1;1	-100	9525	10	8.0

$^*n = n_A + n_B$

The system dynamics were simulated using *ode15s* (Shampine et al., 1999) within MATLAB^{TM}, using an adjusted time step Runge-Kutta method (Cellier and Kofman, 2006). MATLAB^{TM} was used due to its simplicity of developing code. For the solution of the recurring optimal control problem the SQP optimisation algorithm within MATLAB^{TM} is used. The simulations presented in this work were carried out on an HP EliteDesk 800 G2 Desktop Mini PC with an Intel® Core i5-65000 processor with 3.20 GHz and 16.0 GB RAM, running on Windows 7 Enterprise.

2.3. Industrial case study: Nitration of toluene

Additionally to the simple reaction scheme outlined in the previous section, a more complex case study is considered in this work. The nitration of toluene is a relevant process in industry, consisting of endothermic and exothermic reactions (Halder et al., 2008). Thermal runaways can occur still,

Table 3: Process parameters for the nitration of toluene reaction network (Chen et al., 2008; Luo and Chang, 1998; Mawardi, 1982; Sheats and Strachan, 1978).

Reaction i	$k_{0,i}$ $[\mathrm{m^3\,mol^{-1}\,s^{-1}}]$	$E_{a,i}$ $[\mathrm{kJmol^{-1}}]$	$\Delta H_{r,i}$ $[\mathrm{kJmol^{-1}}]$	$n_{1,i}$ $[-]$	$n_{2,i}$ $[-]$
(1)	2.00×10^3	76.5	+30.0	1.00	1.00
(2)	109	12.5	-122	2.27	0.293
(3)	67.3	12.5	-122	2.27	0.293
(4)	5.46	12.5	-122	2.27	0.293

because the process is exothermic overall. The reaction is initiated by the formation of a nitronium ion $\left(NO_2^+\right)$, followed by 3 parallel reactions with toluene (C_7H_8) (Mawardi, 1982):

$$HNO_3 + H_2SO_4 \rightarrow NO_2^+ + HSO_4^- + H_2O \qquad \text{Reaction (1)} \tag{6a}$$
$$NO_2^+ + C_7H_8 + H_2O \rightarrow o - C_7H_7NO_2 + H_3O^+ \qquad \text{Reaction (2)} \tag{6b}$$
$$NO_2^+ + C_7H_8 + H_2O \rightarrow p - C_7H_7NO_2 + H_3O^+ \qquad \text{Reaction (3)} \tag{6c}$$
$$NO_2^+ + C_7H_8 + H_2O \rightarrow m - C_7H_7NO_2 + H_3O^+ \qquad \text{Reaction (4)} \tag{6d}$$

where the letters o-, p- and m- stand for ortho, para and meta positions of the nitronium ion on toluene, respectively. The reactions in Equations (6) are referred to as reactions (1) – (4) hereafter.

Each individual reaction can be described by Arrhenius rate expressions, given by:

$$r_1 = k_{0,1} \exp\left(\frac{-E_{a,1}}{RT_R}\right) [HNO_3]^{n_{1,1}} [H_2SO_4]^{n_{2,1}} \tag{7a}$$
$$r_2 = k_{0,2} \exp\left(\frac{-E_{a,2}}{RT_R}\right) \left[NO_2^+\right]^{n_{1,2}} [C_7H_8]^{n_{2,2}} \tag{7b}$$
$$r_3 = k_{0,3} \exp\left(\frac{-E_{a,3}}{RT_R}\right) \left[NO_2^+\right]^{n_{1,3}} [C_7H_8]^{n_{2,3}} \tag{7c}$$
$$r_4 = k_{0,4} \exp\left(\frac{-E_{a,4}}{RT_R}\right) \left[NO_2^+\right]^{n_{1,4}} [C_7H_8]^{n_{2,4}} \tag{7d}$$

Important to note is that reactions (2) – (4) each produce a H_3O^+ ion, which will combine with HSO_4^- to form H_2SO_4. Hence the sulphuric acid in this reaction network acts as a catalyst. The data used for this reaction network are given in Table 3.

The initial concentrations of each reagent are given by:

$$[\mathrm{HNO_3}]_0 = 6.0\,\mathrm{kmol\,m^{-3}} \tag{8a}$$

$$[\mathrm{H_2SO_4}]_0 = 1.0\,\mathrm{kmol\,m} \tag{8b}$$

$$[\mathrm{C_7H_8}]_0 = 5.5\,\mathrm{kmol\,m^{-3}} \tag{8c}$$

These initial concentrations are used throughout all case studies for the nitration of toluene. The reactor dimensions for this system are given in Table 1.

3. Analysis of Semënov and Routh-Hurwitz criteria

3.1. Batch process with PI control

For the analysis of reliable stability measures in this section a PI controller is used. A PI controller is mathematically described by the following equation:

$$u\left(t\right) = K_P \varepsilon\left(t\right) + \frac{1}{\tau_I}\int_{t_0}^{t_f}\left(\varepsilon\left(t\right)\mathrm{d}t\right) \tag{9}$$

where $u\left(t\right)$ is the control variable given by the coolant flow rate, $\varepsilon\left(t\right)$ is the error at time t given by the temperature deviation, K_P is the proportional constant of the PI controller, and τ_I is the integral constant of the PI controller. K_P and τ_I define how the PI controller behaves for the process, and are set to $K_P = 10\,\mathrm{m^3\,K^{-1}\,s^{-1}}$ and $\tau_I = 1000\,\mathrm{K\,s^2 m^{-3}}$. No systematic tuning methods such as Ziegler-Nichols (Yucelen et al., 2006), Cohen-Coon (Joseph and Olaiya, 2018), or Nyquist (Chen and Seborg, 2003) are applied to the PI controller in this work. The PI controller in this work is used to obtain thermal runaway behaviour. Identifying when each process becomes unstable sets the basis for verifying the reliability of the thermal stability criteria examined.

To analyse how the Semënov and the Routh-Hurwitz criterion behave in a dynamic batch reaction, PI controlled simulations of processes $\mathrm{P}_1 - \mathrm{P}_4$ are considered. To identify where the system becomes unstable and when the criteria identify an unstable system, an initially stable batch reaction is made unstable by a step-wise increase in the reaction set-point temperature. Once the temperature increases uncontrollably, thermal runaway behaviour is obtained. The resulting temperature profiles for processes $\mathrm{P}_1 - \mathrm{P}_4$ are shown in Figure 2.

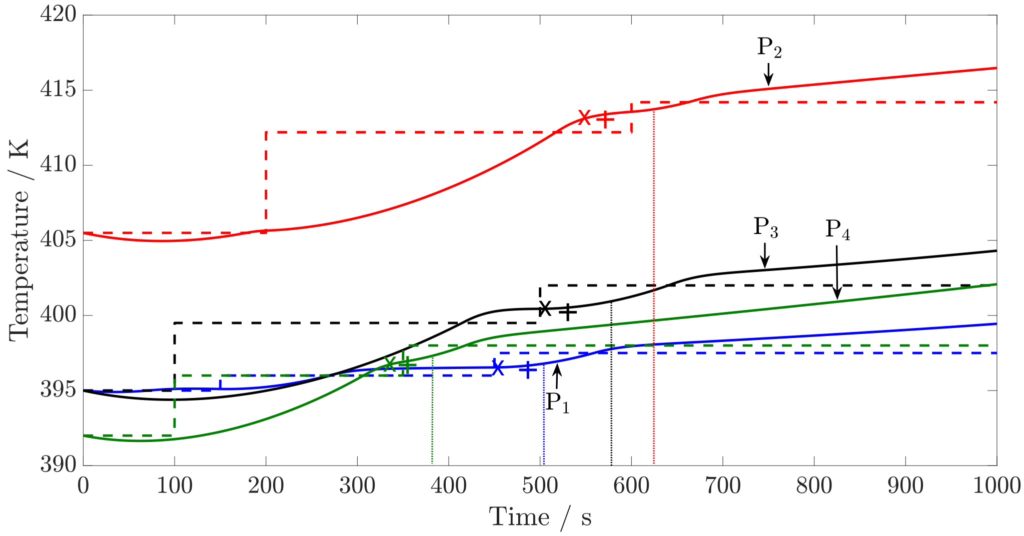

Figure 2: Temperature profiles of PI controlled processes $P_1 - P_4$ with a step-wise increase in reaction set-point temperature. The dashed lines indicate the temperature set-points of the PI controller. The vertical dotted lines show the points in time when each respective process becomes unstable. The x's and +'s indicate when Lyapunov exponents and criterion $\mathcal{K}$ indicate thermal runaway behaviour, respectively.

As can be seen in Figure 2 the temperature profiles initially follow the set-point temperatures. As the set-point temperature increases a second time, each process becomes unstable, resulting in thermal runaway behaviour. The points in time when each process becomes unstable are indicated by vertical dotted lines in Figure 2. These times are identified in the following manner: for each process shown in Figure 2 the same simulation is carried out with a smaller second increase in set-point temperature. The maximum second increase in set-point temperature still resulting in a stable process found. Up until the times indicated by the vertical dotted lines in Figure 2 the two simulations are identical. The times indicated are hence the first points in time for processes $P_1 - P_4$ at which thermal runaway behaviour is unavoidable. It is noted that the cooling valve should have been opened fully before the times indicated by the vertical dotted lines to avoid thermal runaway behaviour.

In the following two sections the reliability of thermal runaway prediction of the Semënov and the Routh-Hurwitz criterion is examined. If no reliable identification of the system stability results, these criteria cannot be used for batch process intensification.

3.2. Semënov criterion

The first quantification of stability occurred in 1940, when the theory of thermal explosions by Semënov was introduced (Semënov, 1940). In this work the heat generation of the reaction system was compared to the available cooling capacity in order to formulate this stability criterion.

Consider the batch reactor system shown in Section 2. In this system heat is generated by an exothermic reaction, denoted by Q_{gen}, and heat is removed with the cooling jacket, denoted by Q_{rem}.

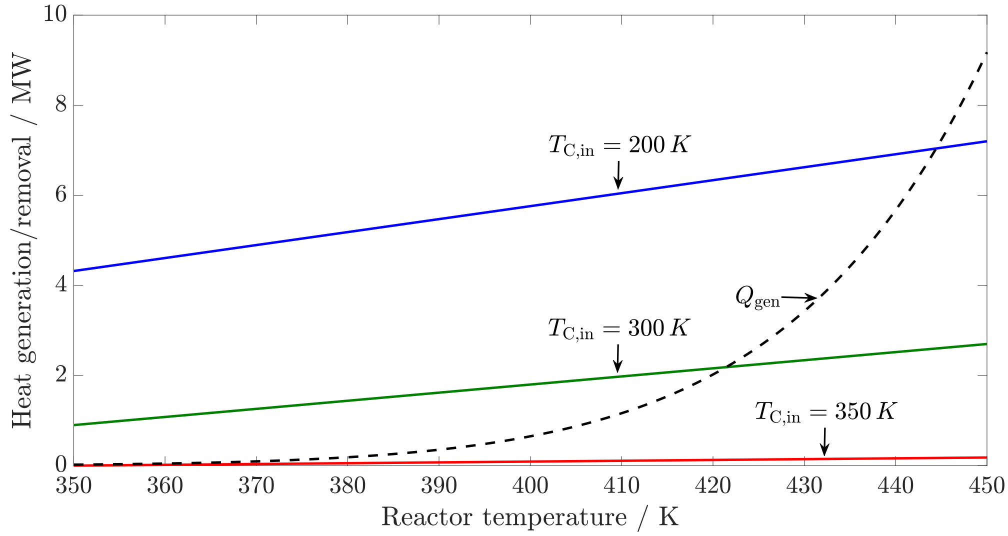

Figure 3: Heat generation (black, dashed line) and heat removal (solid lines) for different coolant inlet temperatures. For the coolant inlet temperatures of 200 K, 300 K, and 350 K, heat transfer coefficient values of 800 $\mathrm{W\,m^{-2}\,K^{-1}}$, 500 $\mathrm{W\,m^{-2}\,K^{-1}}$, and 50 $\mathrm{W\,m^{-2}\,K^{-1}}$, respectively, were used.

The conditions of stability according to Semënov are given by the following two expressions:

$$Q_{\mathrm{gen}} \leq Q_{\mathrm{rem}} \tag{10a}$$

$$\frac{\mathrm{d}Q_{\mathrm{gen}}}{\mathrm{d}t} \leq \frac{\mathrm{d}Q_{\mathrm{rem}}}{\mathrm{d}t} \tag{10b}$$

This can also be represented graphically for an exothermic reaction. Consider a single reaction, as shown in Equation (1), generating heat according to Equation (4), subjected to cooling according to Equation (5). The equations used to analyse how Q_{gen} and Q_{rem} change with reactor temperature are:

$$Q_{\mathrm{gen}} = k_0 \, \exp\left(\frac{-E_a}{R\,T_{\mathrm{R}}}\right) \, [\mathrm{A}]^{n_{\mathrm{A}}} \, [\mathrm{B}]^{n_{\mathrm{B}}} \, (-\Delta H_r)\, V_{\mathrm{R}} \tag{11a}$$

$$Q_{\mathrm{rem}} = U\,A\,(T_{\mathrm{R}} - T_{\mathrm{C}}) \tag{11b}$$

The resulting heat generation and removal rates with respect to reactor temperature, as given in Equation (11), are shown for process P_1 in Figure 3.

The region to the left of the intersection for each solid and the dashed line gives the stable temperature range for the batch reactor at a single point in time. The analysis of stability according to Semënov only gives steady-state results of stability, which is a major limitation.

In Figure 3 several interesting features can be observed: if the coolant inlet temperature is too high, in this case 350 K, then the system is stable only when no heat is generated. As the coolant inlet temperature decreases, the feasible temperature range of operation increases. As the coolant inlet temperature is decreased from 350 K to 300 K and 200 K, the heat transfer coefficient values are increased from 50 $\mathrm{W\,m^{-2}\,K^{-1}}$ to 500 $\mathrm{W\,m^{-2}\,K^{-1}}$ to 800 $\mathrm{W\,m^{-2}\,K^{-1}}$. These values for the heat transfer coefficients are constant and do not vary with temperature. This can be seen by the increase in gradient of the heat removal lines, again increasing the range of feasible reactor temperatures. Once the solid lines in Figure 3 cross the dashed line, the value for Q_{gen} will always be larger than that of Q_{rem} due to the exponential nature of the heat generation. Therefore, once the solid lines and the dashed line cross the stable region of a stationary process can be identified according to Equation (10a). No discussion on the dynamic nature of the process is possible according to Equation (10b) with the results given in Figure 3.

For the verification of the Semënov criterion with respect to dynamic systems, the temperature profiles in Figure 2 are considered. To see how well the Semënov criterion describes the transition to unstable operation, the corresponding profiles of the ratio $Q_{\mathrm{gen}}/Q_{\mathrm{rem,max}}$, where $Q_{\mathrm{rem,max}}$ is the maximum cooling capacity, are plotted in Figure 4.

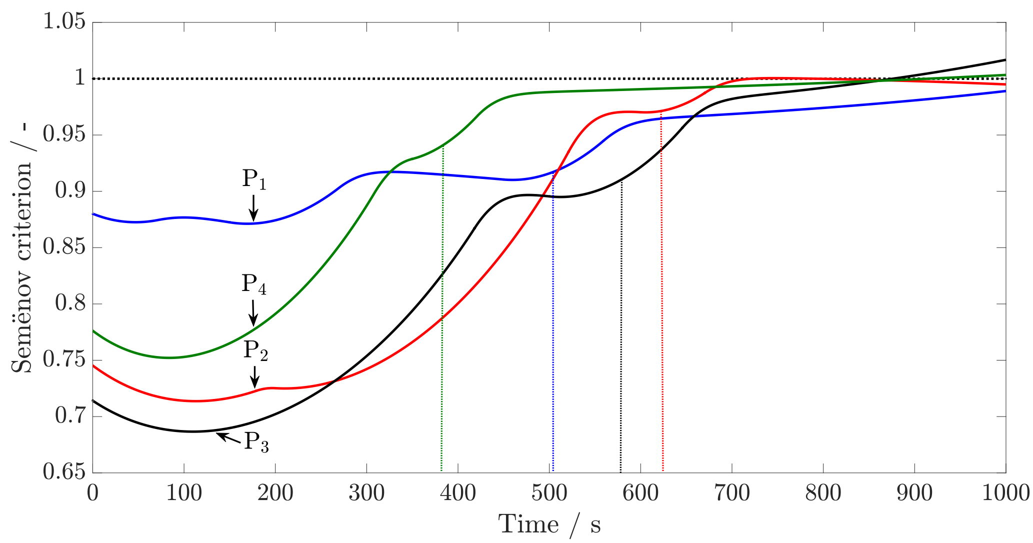

Figure 4: Ratio of heat generation to heat removal, $Q_{\mathrm{gen}}/Q_{\mathrm{rem,max}}$, for processes $\mathrm{P}_1 - \mathrm{P}_4$ shown in Figure 2. The vertical dotted lines show the points in time when each respective process becomes unstable.

The second condition of the Semënov criterion in Equation (10) with respect to heat generation and removal rates, $\frac{\mathrm{d}Q_{\mathrm{gen}}}{\mathrm{d}t}/\frac{\mathrm{d}Q_{\mathrm{rem}}}{\mathrm{d}t}$, is shown for processes $\mathrm{P}_1 - \mathrm{P}_4$ in Figure 5.

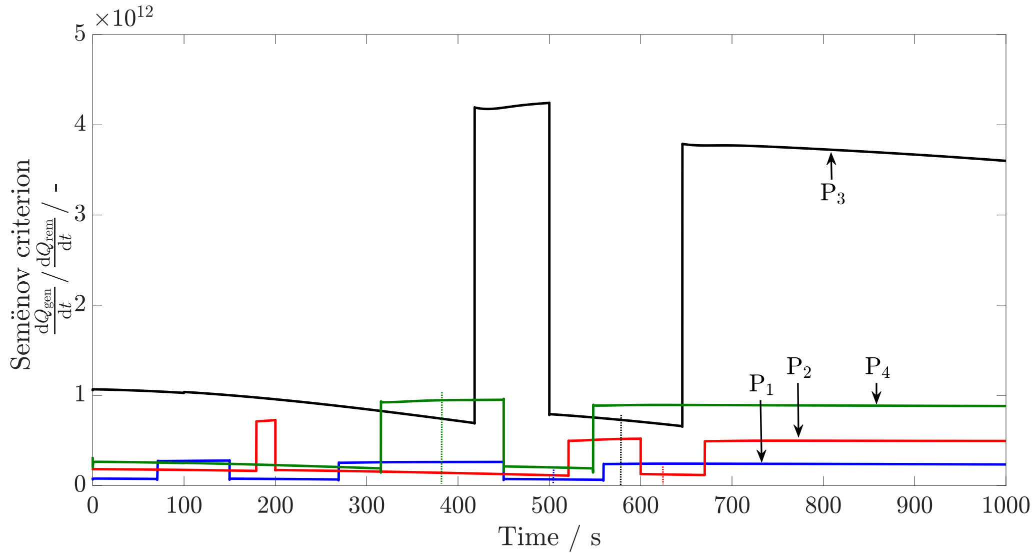

Figure 5: Ratio of heat generation to heat removal rate, $\frac{dQ_{gen}}{dt} / \frac{dQ_{rem}}{dt}$, for processes $P_1 - P_4$, the temperature profiles of which are shown in Figure 2. The vertical dotted lines indicate the points in time when each respective process becomes unstable.

According to Equation (10) an unstable system is present once the system reaches $\frac{Q_{gen}}{Q_{rem,max}} > 1$ and/or $\frac{dQ_{gen}}{dt} / \frac{dQ_{rem}}{dt} > 1$. This means that as long as $\frac{Q_{gen}}{Q_{rem,max}} \leq 1$ and $\frac{dQ_{gen}}{dt} / \frac{dQ_{rem}}{dt} \leq 1$ a stable system is present.

In Figure 4 it is seen that the criterion $\frac{Q_{gen}}{Q_{rem,max}}$ according to Semënov does not give very good predictions of system stability: thermal runaway behaviour occurs while $\frac{Q_{gen}}{Q_{rem,max}} < 1$, as can be seen by the vertical dotted lines showing when thermal runaways occur.

The second condition of the Semënov criterion $\frac{dQ_{gen}}{dt} / \frac{dQ_{rem}}{dt}$ for processes P_1, P_2 and P_4, given in Figure 5, is always smaller than 1 hence predicting stable operation throughout. The value of $\frac{dQ_{gen}}{dt} / \frac{dQ_{rem}}{dt}$ for process P_3 starts larger than 1, drops below 1 and increases abruptly with increases in set-point temperature. Clearly, the profiles for the second Semënov criterion given in Figure 5 do not give a reliable prediction of thermal stability according to Equation (10b).

Therefore using the Semënov criterion for nonlinear, non-steady-state systems would result in unreliable prediction of thermal runaway behaviour.

3.3. Routh-Hurwitz criterion

The Routh-Hurwitz criterion (Anagnost and Desoer, 1991; Hurwitz, 1895; Routh, 1877) uses the Jacobian of the underlying Differential Algebraic Equations (DAEs) to quantify system stability. Hence, in order to use the Routh-Hurwitz criterion, first the Jacobian of the batch reactor equations presented in Section 2 is derived. Consider the following general set of differential equations:

$$\dot{x}_1 = f_1\,(x,\,t) \tag{12a}$$

$$\dot{x}_2 = f_2\,(x,\,t) \tag{12b}$$

$$\vdots \qquad \vdots$$

$$\dot{x}_N = f_N\,(x,\,t) \tag{12c}$$

where N is the number of differential variables x, and $f\,(x,\,t)$ is a generic function depending on x and time t.

For nonlinear systems, a linear approximation of the set of equations can be obtained by using a Taylor series expansion (James et al., 2007). Hence, Equation (12) can be rewritten by the following linear approximation:

$$\dot{x} = \mathbf{J}\,x \tag{13}$$

where $\mathbf{J}$ is the Jacobian matrix including all first order derivatives with respect to x. The entry at row j and column l, J_{jl}, is evaluated by the following expression:

$$J_{jl} = \frac{\partial f_j}{\partial x_l} \tag{14}$$

The eigenvalues of the Jacobian matrix are then found (Chatelin, 2012), giving rise to the stability of the system. If any of the eigenvalues are positive, an unstable system according to the Routh-Hurwitz criterion is present (Routh, 1877; Hurwitz, 1895). Hence, the Routh-Hurwitz criterion for a stable system is given by:

$$\mathrm{eig}\,[\mathbf{J}] \leq 0 \tag{15}$$

where the operator eig $[\mathbf{J}]$ finds the eigenvalues of matrix $\mathbf{J}$.

The performance of this criterion is tested with processes $\mathrm{P}_1 - \mathrm{P}_4$, as was done in Section 3.2 for the Semënov criterion. The temperature profiles for these processes are shown in Figure 2. The system simulated contains 5 differential variables. This leads to the Jacobian to have at most 5 distinct eigenvalues. The linearisation of the system to obtain the Jacobian is carried out in each point in time. This is necessary since a single linearisation cannot capture the whole system dynamics as time proceeds. For clarity, the largest eigenvalue of the Jacobian for each process $\mathrm{P}_1 - \mathrm{P}_4$ is shown as the stability criterion. If the maximum value of all eigenvalues is below zero, a stable system is indicated.

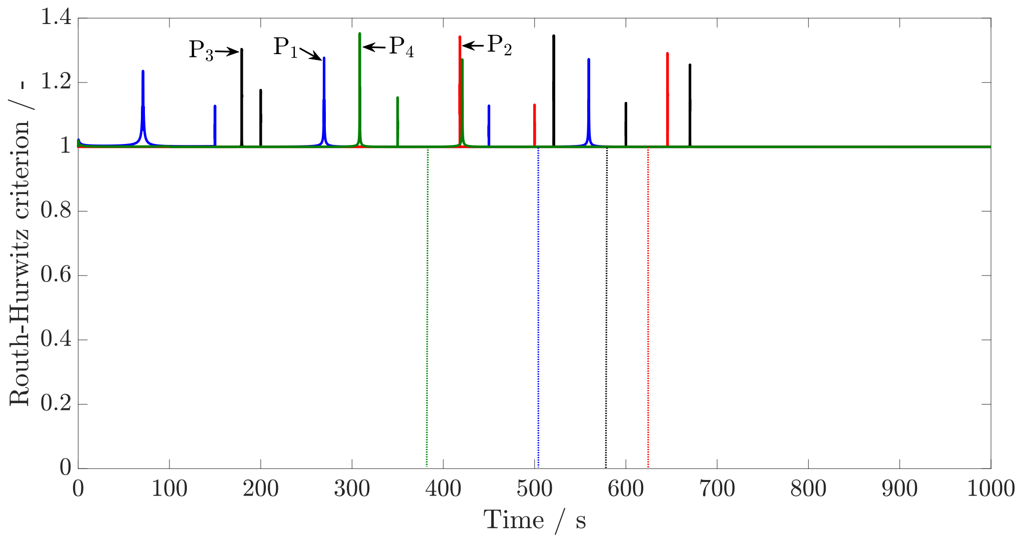

Figure 6: Routh-Hurwitz criterion for processes $P_1 - P_4$. The temperature profiles for these processes are shown in Figure 2. The vertical dotted lines show the points in time when each respective process becomes unstable.

The transition from stable to unstable operation has to be identified with this criterion in order to show its reliability. The resulting Routh-Hurwitz criterion profiles for processes $P_1 - P_4$ are shown in Figure 6.

In Figure 6 it is seen that for each process unstable operation is predicted throughout. This is wrong because initially every process is under control due to the PI controller present. Only after the second increase in set-point temperature does each process become unstable. Since batch reactors are never at steady-state, the Routh-Hurwitz criterion gives an unreliable stability prediction for these types of systems. Therefore a different stability criterion is required for this purpose.

3.4. Thermal stability criteria for batch processes

As outlined in the introduction, two reliable thermal stability criteria exist in the literature for batch processes: criterion $\mathcal{K}$ and Lyapunov exponents. A brief background on each thermal stability measure is given here for completeness.

Thermal stability criterion $\mathcal{K}$ is based on the divergence criterion (Bosch et al., 2004). Since the divergence criterion is too conservative (Kähm and Vassiliadis, 2018d) a correction function $\mathcal{E}$ is introduced. The correction function $\mathcal{E}$ predicts the divergence at the boundary of stability, hence resulting in the following equation for criterion $\mathcal{K}$:

$$\mathcal{K} = \text{div}\left[\mathbf{J}\right] - |\mathcal{E}| \tag{16}$$

If the value of $\mathcal{K}$ becomes positive, an unstable process is identified. More detail on the derivation of criterion $\mathcal{K}$ and the correction function $\mathcal{E}$ can be found in Kähm and Vassiliadis (2019).

Lyapunov exponents, on the other hand, require a parallel simulation to be carried out. For each state variable x the nominal trajectory is perturbed at initial time t_0 by a small positive amount δx. The distance between the trajectories is measured after a certain time frame t_{lyap} in the following manner:

$$\Lambda(t_0, x_0) = \frac{1}{t_{\text{lyap}}} \ln \left(\frac{|x\left(t_0 + t_{\text{lyap}}, x_0 + \delta x\right) - x\left(t_0 + t_{\text{lyap}}, x_0\right)|}{\delta x} \right) \tag{17}$$

If the Lyapunov exponent in Equation (17) becomes positive, an unstable process is predicted. A more detailed discussion on how Lyapunov exponents are used and how values for t_{lyap} and δx are determined can be found in Kähm and Vassiliadis (2018b).

3.5. Discussion of results

The Semënov criterion and Routh-Huriwtz criterion work well in identifying the stability of continuous processes with a clear stationary point, *e.g.* for CSTRs. From the stability criterion profiles in Sections 3.2 and 3.3 it is clear that these criteria do not give reliable predictions of thermal stability in batch processes. As mentioned in the introduction, this also means that the Barkelew, Balakotaiah, Baerns and Frank-Kamenet͡skiĭ criteria are not applicable to batch processes either. The +'s and x's in Figure 2 indicate when criterion $\mathcal{K}$ and Lyapunov exponents identify thermal runaway behaviour, respectively. As can be seen, the thermal runaway predictions are before the actual loss of thermal stability hence giving a degree of conservativeness. Nevertheless, criterion $\mathcal{K}$ and Lyapunov exponents result in reliable thermal runaway prediction (Kähm and Vassiliadis, 2018b,c). Hence in the further analysis of robust thermal stability criteria only Lyapunov exponents and criterion $\mathcal{K}$ are considered.

4. Robustness of criterion $\mathcal{K}$ and Lyapunov exponents

The accuracy of a stability criterion is of utmost importance when the system state is close to the boundary of instability. Hence, the sensitivity with respect to parametric uncertainty of thermal stability criterion $\mathcal{K}$ and Lyapunov exponents is investigated for process P_5 controlled by a PI controller in similar manner to processes $\mathrm{P}_1 - \mathrm{P}_4$. The resulting temperature profile of process P_5 is shown in Figure 7.

To adequately compare parameters and the effect of uncertainty, a 95% confidence region for each parameter is assumed. This gives the region where the Lyapunov exponent and criterion $\mathcal{K}$ for the system would lie 95% of the time if each parameter (a normally distributed random variable) was sampled many times. The comparison of the confidence regions allows the comparison of the impact between parameters.

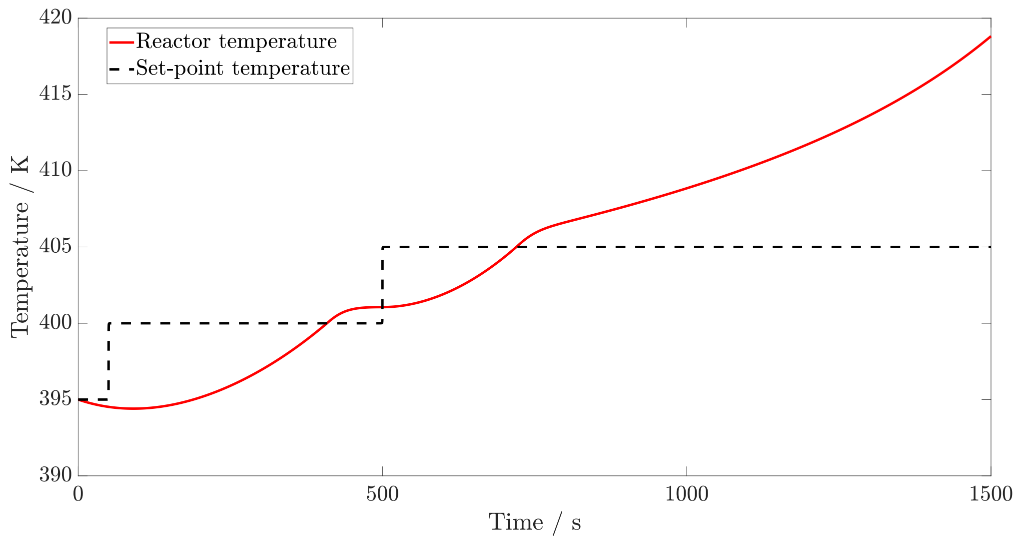

Figure 7: Temperature profiles of PI controlled process P_5 with a step-wise increase in reaction set-point temperature. The dashed line indicate the temperature set-point of the PI controller.

It is assumed that uncertainties in the reactor and cooling jacket volumes, as well as the heat transfer area are known well enough such that they are 100% certain. The order of reaction is assumed to be restricted to integers. Process disturbances as well as measurement noise are not considered at this stage. Therefore, confidence intervals of $\mathcal{K}$ and Lyapunov exponents were calculated for the following model parameters: ρ_{R}, ρ_{C}, $C_{p,\mathrm{R}}$, $C_{p,\mathrm{C}}$, k_0, E_{a}, ΔH_{r}, and U. For all but one, a relative standard error (RSD) of 5% was used as an upper limit of an acceptable empirical result. An exception had to be made for the activation energy E_a with 1% RSD being used. The fact that the activation energy appears within an exponential for the reaction rate (Equation (2)) means deviations of 5% RSD would result in extremely different system behaviour.

In Section 2 it is assumed that strong mixing is present in all processes. This is equivalent to assuming infinitely large diffusion coefficient values. For a complete consideration of parametric uncertainty the uncertainty in diffusion coefficients would have to be included as well. This would only be necessary if uncertainty in diffusion coefficients might result in non-turbulent mixing. In industry turbulent mixing can be guaranteed for reacting mixtures with a low and known viscosity. Therefore in this work parametric uncertainty with respect to diffusion coefficients is omitted.

The probability distribution used for the analysis of robustness with respect to the enthalpy of reaction ΔH_r for process P_5 is given by:

$$\Delta H_r \sim \mathcal{N}\left(\mu_{\Delta H_r}, \sigma^2_{\Delta H_r}\right) \tag{18a}$$

where $\mu_{\Delta H_r}$ is the mean and $\sigma_{\Delta H_r}$ is the standard deviation of ΔH_r, given numerically by:

$$\mu_{\Delta H_r} = -100\,\mathrm{kJ\,mol^{-1}} \tag{18b}$$

$$\sigma_{\Delta H_r} = 2.55\,\mathrm{kJ\,mol^{-1}} \tag{18c}$$

The standard deviation is obtained in the following manner: for 95% certainty in the mean value of the enthalpy of reaction given a 10% range, equivalent to 5% RSD, the z-value of a normal distribution is given by (Rasmussen and Williams, 2006):

$$1.96 = \frac{0.95\mu_{\Delta H_r} - \mu_{\Delta H_r}}{\sigma_{\Delta H_r}} \tag{19a}$$

$$\sigma_{\Delta H_r} = \frac{-0.05\mu_{\Delta H_r}}{1.96} \tag{19b}$$

$$\sigma_{\Delta H_r} = 2.55\,\mathrm{kJ\,mol^{-1}} \tag{19c}$$

The normal distribution parameters for all remaining parameters are evaluated in a similar manner, and summarised in Table 4. These values are used for all the sensitivity analyses for criterion $\mathcal{K}$ and Lyapunov exponents in the following sections.

Table 4: Normal distribution parameters for all uncertain parameters.

	ΔH_r $\left[\frac{\mathrm{kJ}}{\mathrm{mol\,s}}\right]$	E_a/R [K]	$k_0 \times 10^{-3}$ $\left[\frac{\mathrm{m^3}}{\mathrm{kmol\,s}}\right]$	U $\left[\frac{\mathrm{W}}{\mathrm{m^2\,K}}\right]$	ρ_R $\left[\frac{\mathrm{kg}}{\mathrm{m^3}}\right]$	ρ_C $\left[\frac{\mathrm{kg}}{\mathrm{m^3}}\right]$	$C_{p,\mathrm{R}}$ $\left[\frac{\mathrm{kJ}}{\mathrm{kg}}\right]$	$C_{p,\mathrm{C}}$ $\left[\frac{\mathrm{kJ}}{\mathrm{kg}}\right]$
μ	-100	9525	300	600	950	1000	2330	4180
σ	2.55	48.6	7.65	15.3	24.2	25.5	59.4	107

4.1. Effect of parametric uncertainty on criterion $\mathcal{K}$

Figure 8 shows results for the reaction mixture density, which equally hold for the reaction mixture heat capacity. It can be seen that the impact of the parameters on the stability criterion $\mathcal{K}$ changes depending on the system state. It follows from Equation (4) that a reduction in the reaction mixture density/heat capacity increases the magnitude of the rate of change of reactor temperature. The change in sign of the rate of change of temperature is closely associated with a transition to thermal instability thus causing the behaviour observed. Based on low sensitivity of $\mathcal{K}$ to the reaction mixture density/heat capacity at the boundary of instability and the fact these properties can be measured easily with good accuracy, density and heat capacities are not considered further.

Results for the enthalpy change of reaction and the pre-exponential constant are presented in

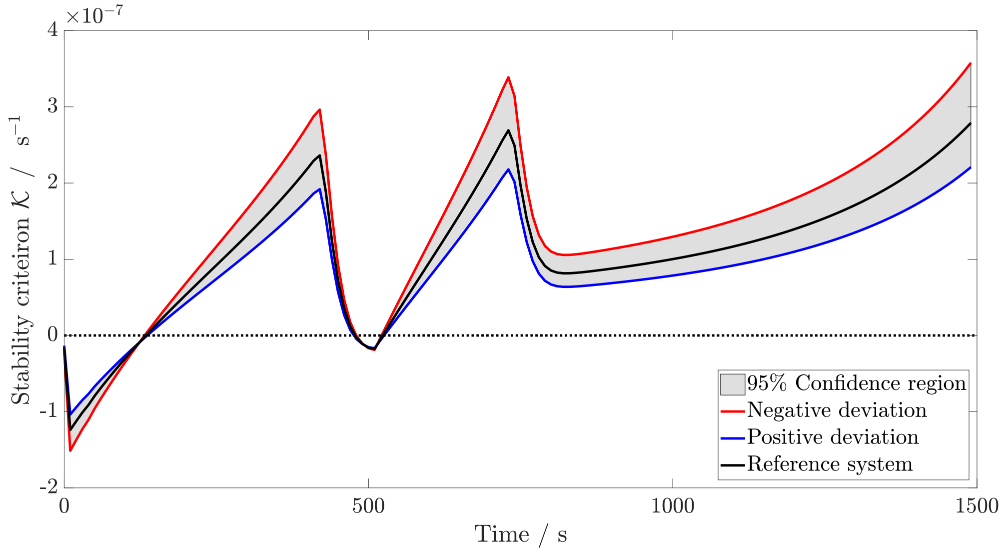

Figure 8: Sensitivity of the stability criterion $\mathcal{K}$ to uncertainty in reaction mixture density, ρ_{R}, with 5% RSD. Identical results were obtained for reaction mixture heat capacity $C_{p,\mathrm{R}}$.

Figures 9 and 10. It can be seen that the uncertainties in the two parameters have near identical impacts on the stability criterion $\mathcal{K}$. This observation is explained by the similarities in their contributions to system behaviour, in particular to the rate of heat generation, as seen in Equation (11a).

Results for the heat transfer coefficient are shown in Figure 11. Sensitivity of $\mathcal{K}$ with respect to the heat transfer coefficient U is observed to vary significantly depending on the runaway potential of the current system state. This feature is explained by the reduction in the fraction of heat being removed from the system as thermal runaway proceeds, which is evident from Equation (5).

In Figure 12 the results for the activation energy are shown. Despite a smaller RSD being used, the most significant effect on criterion $\mathcal{K}$ is observed for uncertainty in the activation energy. This is the case because the rate of heat generation is proportional to the exponential of E_{a}, as mentioned previously. The high sensitivity observed indicates that for stability criterion $\mathcal{K}$ to be reliable, activation energy of the reaction has to be known with high accuracy.

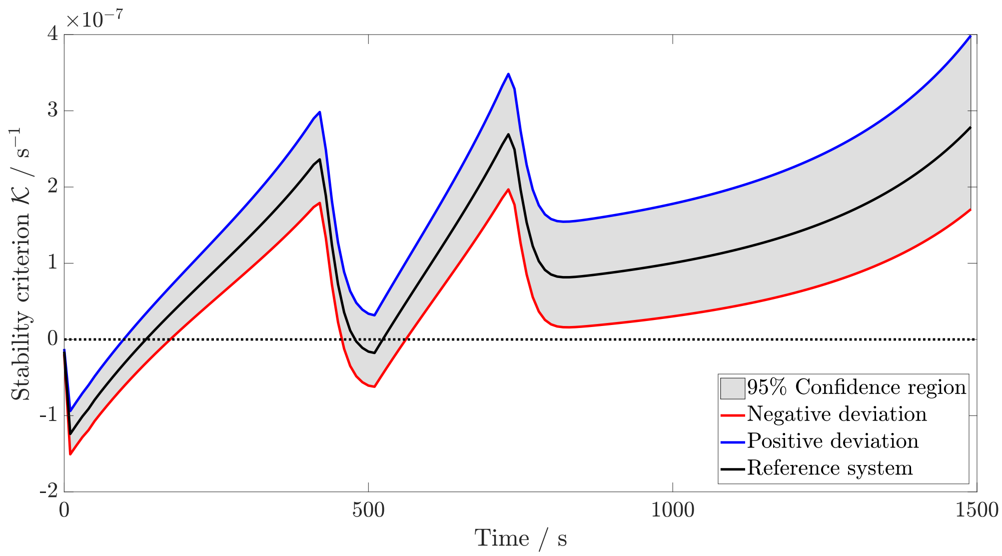

Figure 9: Sensitivity of the stability criterion $\mathcal{K}$ to uncertainty in the pre-exponential constant, ΔH_r, with 5% RSD.

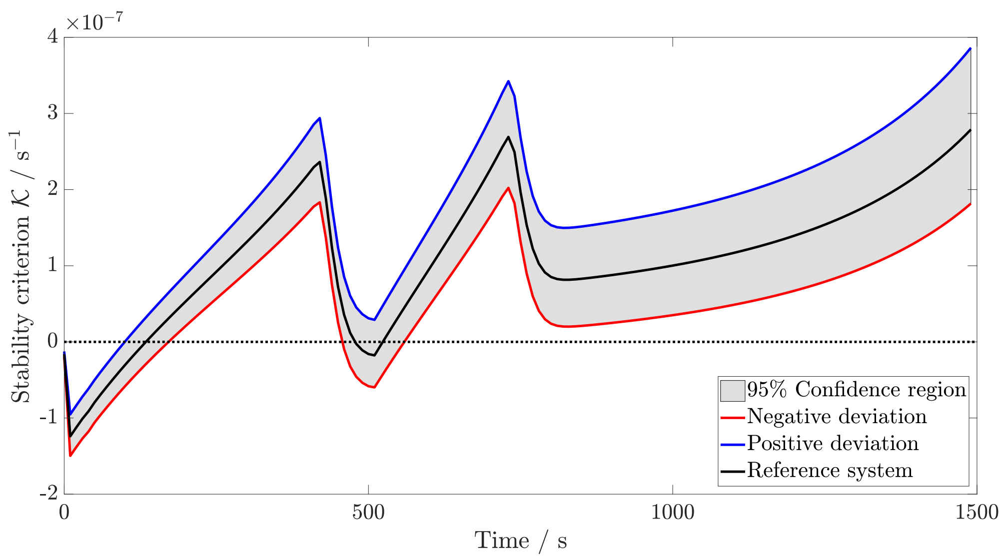

Figure 10: Sensitivity of the stability criterion $\mathcal{K}$ to uncertainty in the Arrhenius pre-exponential factor, k_0, with 5% RSD.

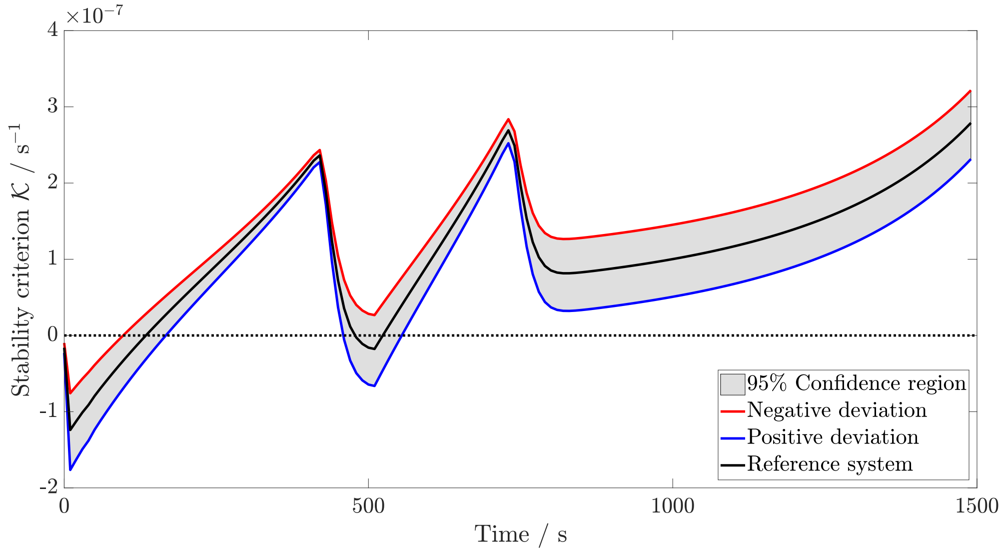

Figure 11: Sensitivity of the stability criterion $\mathcal{K}$ to uncertainty in the heat transfer coefficient, U, with 5% RSD.

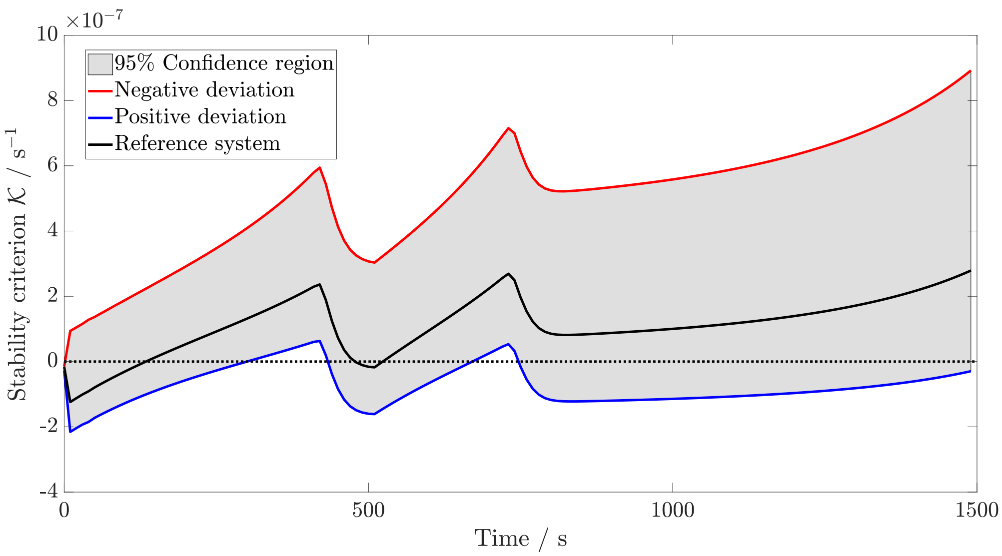

Figure 12: Sensitivity of the stability criterion $\mathcal{K}$ to uncertainty in the activation energy, E_{a}, with 1% RSD.

Based on the above results it is identified that there are four parameters with the most significant impact on the stability criterion $\mathcal{K}$: the activation energy, E_{a}, the enthalpy change of reaction, ΔH_{r}, the Arrhenius pre-exponential factor, k_0, and the heat transfer coefficient, U.

4.2. Effect of parametric uncertainty on Lyapunov exponents

As done for criterion $\mathcal{K}$, the effect of uncertainty in the reaction mixture heat capacity on the Lyapunov exponents is considered first. For this purpose, the same normal distributions and standard deviations as outlined in Table 4 are used. The profiles of the Lyapunov exponent with respect to temperature, $\Lambda_{\text{lyap},T}$, with respect to uncertainty in ρ_{R} and $C_{p,\text{R}}$ for an RSD of 5% is shown in Figure 13.

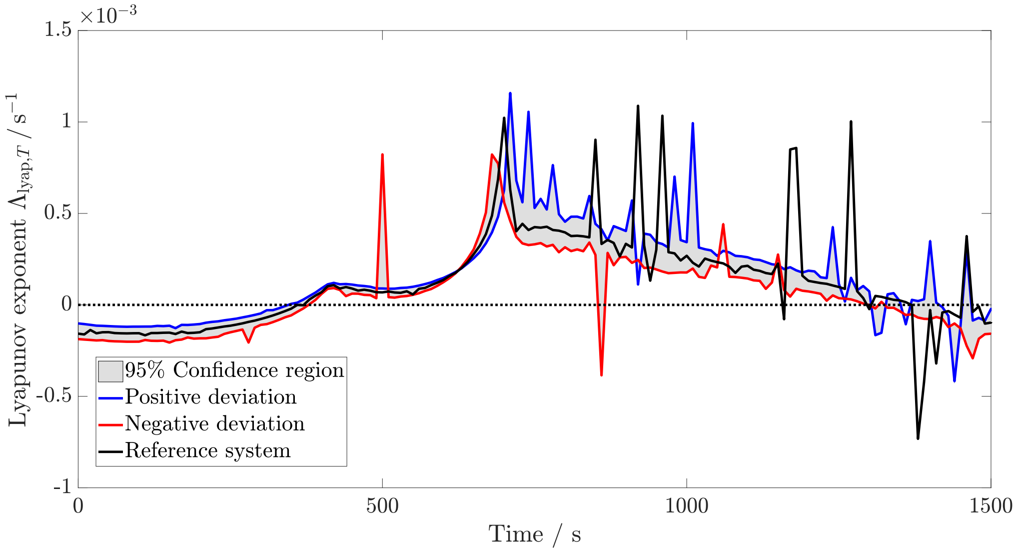

Figure 13: Sensitivity of the Lyapunov exponent with respect to reactor temperature, $\Lambda_{\text{lyap},T}$ to uncertainty in reaction mixture heat capacity, $C_{p,\text{R}}$, with 5% RSD. Identical results were obtained for reaction mixture density ρ_{R}.

As observed for criterion $\mathcal{K}$, uncertainty in the reaction mixture heat capacity, as well as density, has little effect on the Lyapunov exponent values. The points in time when instability is predicted only varies to a negligible extent. Therefore, these parameters are excluded for the further analysis of uncertainty for Lyapunov exponents.

The effect of uncertainty in the enthalpy of reaction and the Arrhenius pre-exponential factor on Lyapunov exponents, each with 5% RSD, is shown in Figure 14 and 15.

Similarly to the results for criterion $\mathcal{K}$, uncertainty in the reaction enthalpy and the Arrhenius pre-expontnial influence the Lyapunov exponent in a nearly identical manner. As was described for criterion $\mathcal{K}$, this is due to the form in which these parameters appear in the overall energy balance of the system, given in Equation (4). The effect of uncertainty in these two parameters is hence important when considering robust MPC techniques.

How uncertainty in the heat transfer coefficient effects thermal stability prediction using Lyapunov exponents is shown in Figure 16.

In Figure 16 it is seen that uncertainty in the heat transfer coefficient U significantly affects the predictions made by Lyapunov exponents about system stability. The smaller the value of the heat transfer coefficient used with Lyapunov exponents, the earlier unstable system behaviour is predicted. This is the case, because a smaller heat transfer coefficient results in less cooling.

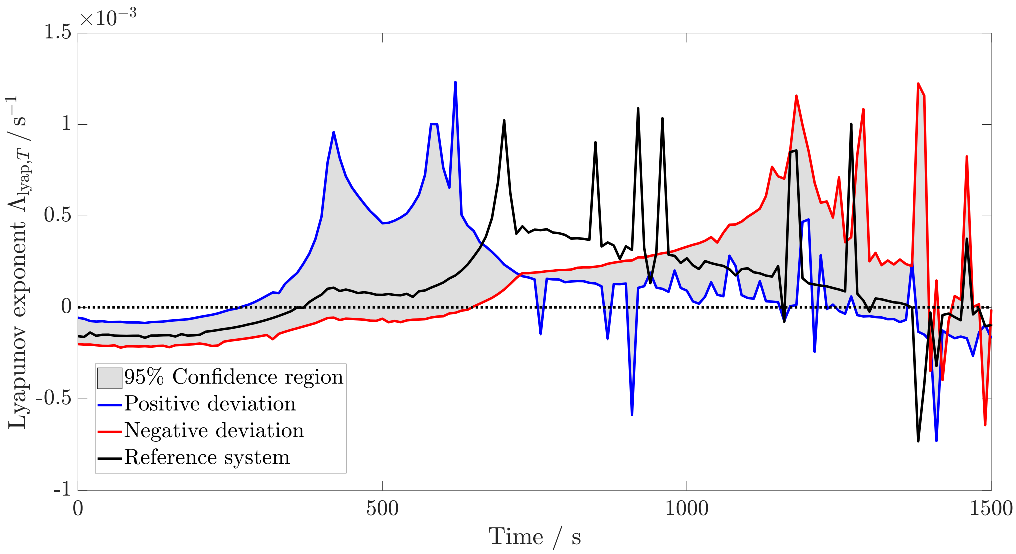

Figure 14: Sensitivity of the Lyapunov exponent with respect to reactor temperature, $\Lambda_{\mathrm{lyap},T}$ to uncertainty in enthalpy of reaction, ΔH_r, with 5% RSD.

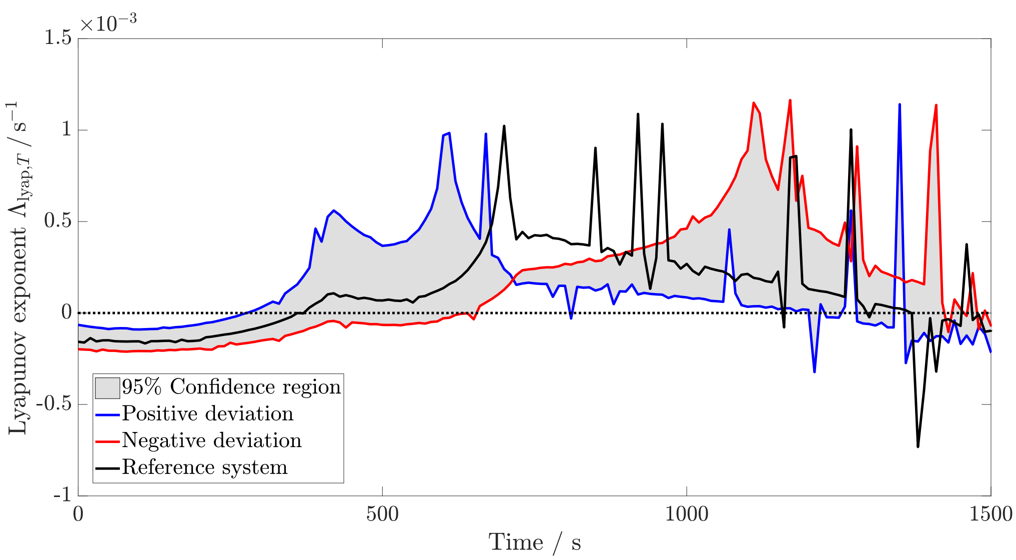

Figure 15: Sensitivity of the Lyapunov exponent with respect to reactor temperature, $\Lambda_{\mathrm{lyap},T}$ to uncertainty in Arrhenius pre-exponential factor, k_0, with 5% RSD.

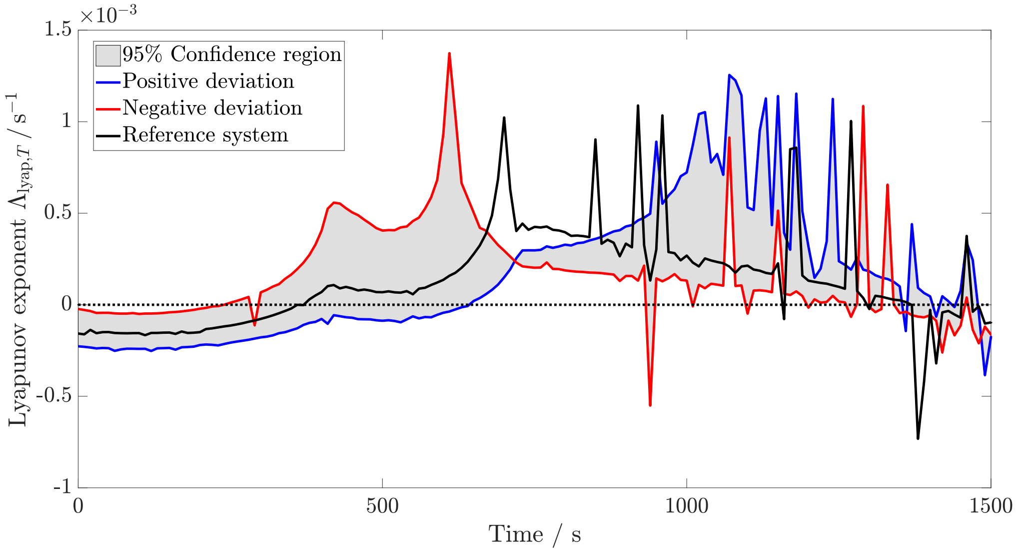

Figure 16: Sensitivity of the Lyapunov exponent with respect to reactor temperature, $\Lambda_{\text{lyap},T}$ to uncertainty in heat transfer coefficient, U, with 5% RSD.

Lastly, the effect of uncertainty in the activation energy is considered. Again, 1% RSD is used because a deviation of 5% RSD, as was done for all other parameters, would result in extremely different system dynamics. Such large deviations would not be beneficial when considering the use of robust MPC techniques. The profiles for the Lyapunov exponents with respect to deviated activation energy values are shown in Figure 17.

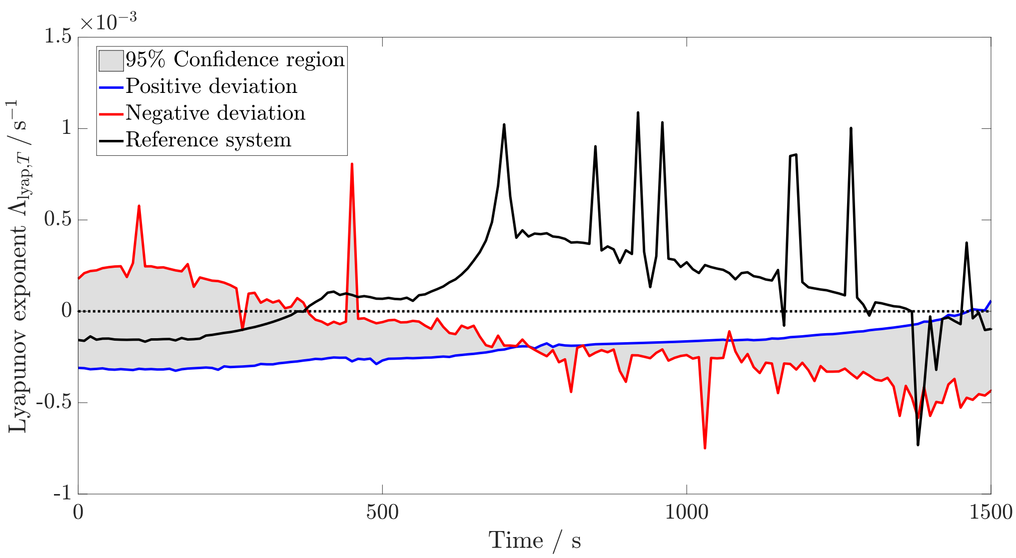

Figure 17: Sensitivity of the Lyapunov exponent with respect to reactor temperature, $\Lambda_{\text{lyap},T}$ to uncertainty in activation energy, E_a, with 1% RSD.

As expected, even a 1% RSD results is large deviations in the Lyapunov exponent value. Important to note is that a negative deviation results in faster reaction dynamics. A negative deviation of 1% RSD results in the initial operating point being classified as unstable. A positive deviation of 1% RSD only results in thermal runaway prediction at the end of the time frame considered in the simulation. Hence, the value of the activation energy should be known to a high degree of accuracy, confirming the results obtained for criterion $\mathcal{K}$.

4.3. Results of sensitivity analysis

From the analysis of parametric uncertainty above for criterion $\mathcal{K}$ and Lyapunov esponents, similar results are obtained:

1. uncertainty densities and heat capacities have a negligible effect on thermal stability prediction
2. uncertainty in the enthalpy of reaction, Arrhenius pre-exponential factor, and heat transfer coefficient are included with a deviation of 5% RSD within the 95% confidence interval
3. the value of activation energy has to be known to a high degree to obtain a sensible range of potential system behaviours. Hence, a deviation of 1% RSD within the 95% confidence interval is used

The following section will use these results to formulate robust MPC frameworks using uncertainty in the outlined parameters embedded with thermal stability prediction.

5. Process intensification with robust MPC

Intensifying batch processes can be achieved by constantly increasing the reactor temperature during the process. This results in shorter reaction times to achieve a certain target conversion. While the reactor temperature is increased, the process must not enter an unstable regime. Such a stability constraint can be embedded within an MPC framework and cannot be achieved with PID control.

Model Predictive Control (MPC) is a control formulation which allows the addition of system constraints, as well as an objective to be optimised. At every MPC step an Optimal Control Problem (OCP) is solved. This OCP involves a control horizon t_c and a prediction horizon t_p. During the control horizon a specified number of control steps are free to vary in order to satisfy the system constraints and optimise the objective. Beyond the control horizon and within the prediction horizon the last control input found is assumed to be applied.

The MPC algorithm is largely defined by the control horizon t_c and the prediction horizon t_p. The control horizon sets the time frame over which the MPC algorithm finds the optimal control inputs such that the system follows a given reference trajectory. The prediction horizon is used to simulate the model used for MPC to predict how the system will behave for the control inputs found, assuming the last control input within the control horizon is kept constant. The MPC framework used in this work uses a control horizon of $t_c = 30$ s with 3 control steps of same length, and a prediction horizon of $t_p = 70$ s. Since only the first control step is implemented after which the optimisation procedure is repeated, the algorithm has 10 s to evaluate the optimal sequence of control inputs. This presents an upper bound on the computational time which must not be exceeded.

The intensification of batch processes requires the full nonlinear model as there is no steady-state operating point. This condition presents issues with respect to defining stable operating points, which is why a different solution to this issue is required. In Kähm and Vassiliadis (2018a,b,c,d) it is shown how stability criteria can be incorporated into standard MPC frameworks as nonlinear constraints. To account for uncertainty within the system, two robust MPC frameworks are considered here: scenario-based MPC and worst case MPC.

For completeness, the nonlinear constraints embedded within MPC are given by:

$$\mathcal{K} \leq 0 \tag{20a}$$

$$\Lambda_{\text{lyap}} \leq 0 \tag{20b}$$

where in Equation (20b) all relevant Lyapunov exponents are included. Only one of the constraints given in Equation (20) is used at one time. If, at any time, the constraint used becomes positive, an unstable process is identified. More details of how Lyapunov exponents and criterion $\mathcal{K}$ are evaluated for the use with MPC can be found in Kähm and Vassiliadis (2018b) and Kähm and Vassiliadis (2018c), respectively.

The nitration of toluene is used as the case study for the robust MPC frameworks. The MPC frameworks embedded with criterion $\mathcal{K}$ and Lyapunov exponents are compared by considering the effect on stability, intensification and computational time. The initial temperature of the process is set to 450 K. The main product is chosen to be o-nitrotoluene, with a target concentration of $2.5\,\text{kmol}\,\text{m}^{-3}$. Sample temperature and concentration profiles of batch process intensification for the nitration of toluene using MPC embedded with Lyapunov exponents are shown in Figure 18, taken from Kähm and Vassiliadis (2018b).

As can be seen in Figure 18, process intensification using MPC with measures of thermal stability enable a continuous increase in reactor temperature until the upper temperature limit is reached. Any process exceeding the maximum temperature is considered as unstable in the following analysis.

5.1. Scenario-based MPC

In the previous section it was shown that uncertainty in the enthalpy of reaction, Arrhenius pre-exponential factor, activation energy and heat transfer coefficient indeed affect the prediction of thermal

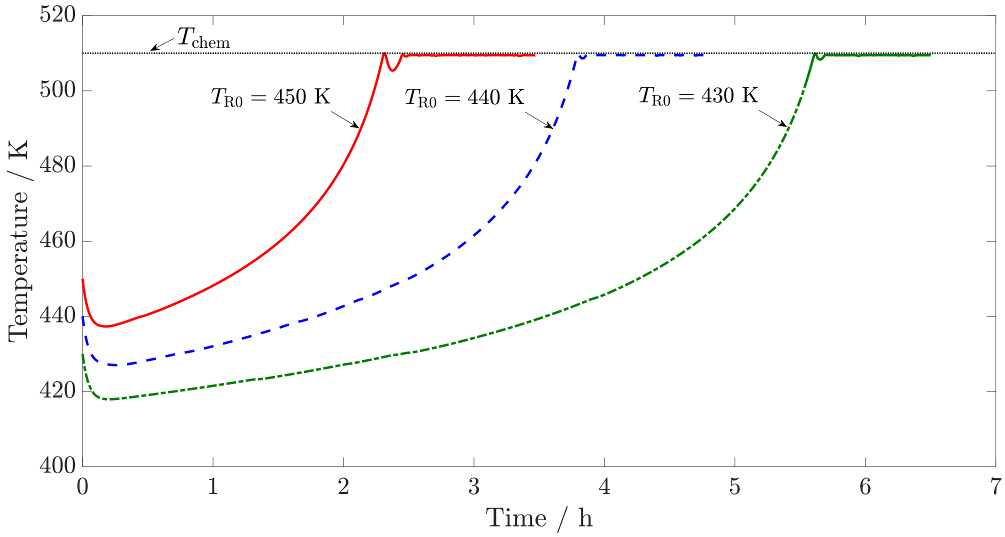

(a) Temperature profiles for intensified processes of the nitration of toluene. The solid line relates to initial temperatures of $T_{\text{R0}} = 450$ K, the dashed line relates to $T_{\text{R0}} = 440\,\text{K}$ and the dash-dotted line relates to $T_{\text{R0}} = 430$ K. The dotted line indicates the maximum allowable temperature of $T_{\text{chem}} = 510$ K.

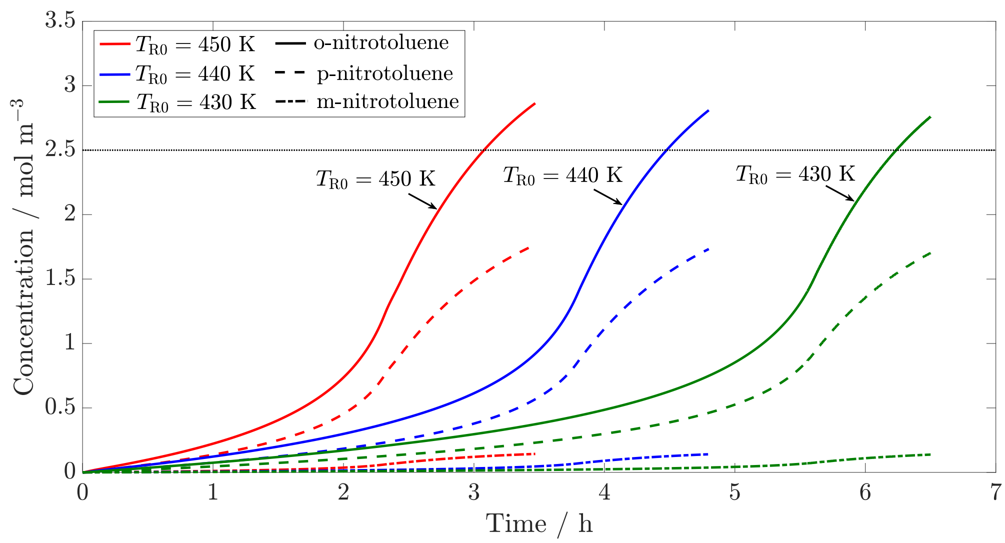

(b) Concentration profiles for the nitration of toluene reaction system. The profiles are obtained by control with MPC framework 1. The dotted line indicates the target concentration for o-nitrotoluene.

Figure 18: Results for the intensification of the nitration of toluene using MPC embedded with Lyapunov exponents at different starting temperatures T_{R0} (Kähm and Vassiliadis, 2018b).

stability using criterion $\mathcal{K}$ and Lyapunov exponents. To ensure safe operation of industrial processes, it is therefore of utmost importance that the MPC framework employed takes this uncertainty into consideration.

As was discussed in the introduction, several methods of dealing with parametric uncertainty exist in the literature. In a similar manner to the analysis in Section 4, several sets of parameters can be sampled from normal distributions of each individual parameter. For each set of parameters a scenario is created, which is included within the MPC framework. This method is called *scenario-based* MPC.

Unlike standard formulations of MPC problems (Rawlings and Mayne, 2015; Christofides et al., 2011) the optimisation and constraints of the MPC algorithm are not considered for the nominal model, but for several scenarios with sampled parameter values. Hence, the modified formulation is as follows:

$$\min_{u} \sum_{z=1}^{100} \int_{t_0^{(s)}}^{t_0^{(s)}+t_p} \Phi_z \, \mathrm{d}t \tag{21a}$$

subject to:

$$\begin{aligned} f_z\left(x, y_z, u, t\right) &= \dot{x} & \quad z = 1, 2, \ldots, S \quad & (21b) \\ h_z\left(x, y_z, u, t\right) &= 0 & \quad z = 1, 2, \ldots, S \quad & (21c) \\ g_z\left(x, y_z, u, t\right) &\leq 0 & \quad z = 1, 2, \ldots, S \quad & (21d) \\ t_0^{(s)} \leq t^{(s)} &\leq t_0^{(s)} + t_p & & (21e) \end{aligned}$$

where the subscript z indicates each individual scenario, Φ_z is the objective function for each scenario, and it is assumed that S scenarios are simulated for each MPC step (s).

Thermal stability criterion $\mathcal{K}$ and Lyapunov exponents are used as stability criteria for the MPC formulation in Equation (21). The performance of scenario-based MPC is investigated using the nitration of toluene. The implementation of scenario-based MPC is schematically shown in Figure 19.

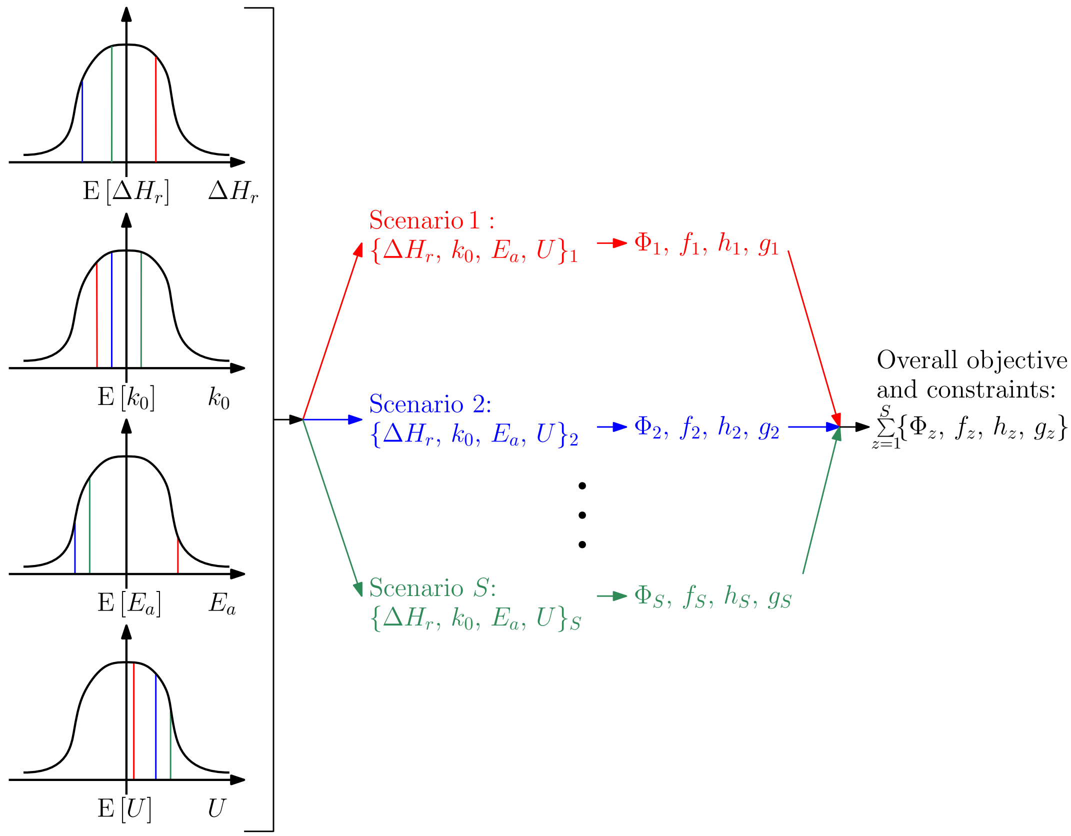

Figure 19: Schematic showing scenario-based MPC with sampling of parameter values to obtain the overall problem solved by the MPC algorithm.

The performance of scenario-based MPC embedded with criterion $\mathcal{K}$ and Lyapunov exponents is assessed by simulating the nitration of toluene for different numbers of scenarios, each using a sample of parameters ΔH_r, k_0, E_a and U according to Figure 19.

As the number of scenarios increases, the number of parameter sets samples increases. Therefore, with an increasing number of scenarios it is more likely to obtain a set of parameters which would result in a more unstable system than the real system being controlled. The MPC framework is required to ensure that each scenario with its set of sampled parameters is stable. Therefore, as the number of scenarios increases, the probability of the MPC framework having to control more unstable processes than the nominal system increases. Hence, it is expected that the number of simulations resulting in thermal runaway behaviour decreases as the number of scenarios increases.

100 simulations are carried out with 1, 2, 3, 5, 8 and 10 scenarios for the nitration of toluene using MPC embedded with criterion $\mathcal{K}$ and with Lyapunov exponents. The fraction of processes that are unstable with this control scheme for each number of scenarios S is shown in Figure 20.

When using 3 or more scenarios a reduction of thermal runaway behaviour to 0% is achieved with criterion $\mathcal{K}$. Lyapunov exponents embedded within the scenario-based MPC framework results in no

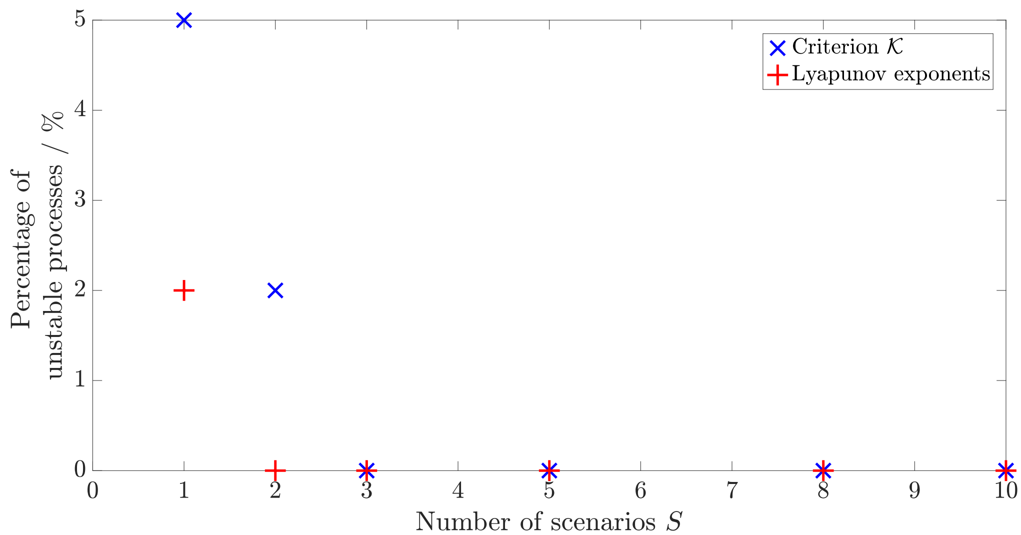

Figure 20: Fraction of simulations for the nitration of toluene resulting in thermal runaway behaviour for each number of scenarios. The percentages are evaluated based on 100 simulations carried out for each control scheme.

thermal runaways if 2 or more scenarios are included. As previously mentioned, these percentages are taken from 100 simulations carried out for each stability criterion embedded within MPC. Important to note is that using 3 or more scenarios does not guarantee stable operation without thermal runaway behaviour. In this work only 100 simulations are carried out, based on which the percentage of thermal runaway reactions are found. If a larger number of processes are to be carried out it is expected that thermal runaway behaviour will occur even when using more than 3 scenarios.

The processing times t_{reac} to reach the target concentration of o-nitrotoluene of $2.5\,\text{kmol}\,\text{m}^{-3}$ are shown in Figure 21.

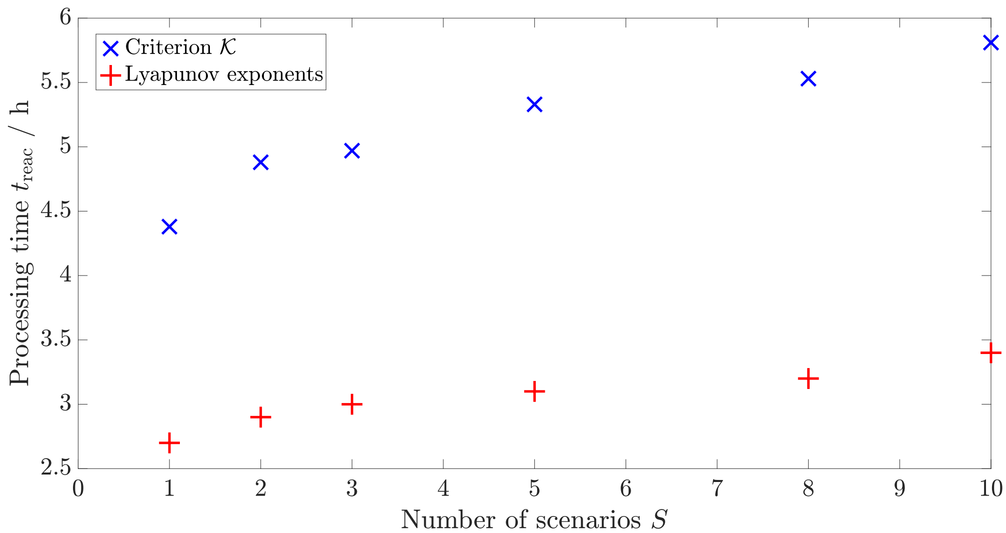

Figure 21: Processing times t_{reac} to reach the target concentration of o-nitrotoluene for the nitration of toluene with each number of scenarios.

As the number of scenarios increases, the time required to reach the final concentration increases. Compared to the deterministic results for the intensification of nitration of toluene with initial temperature of 450 K shown in Kähm and Vassiliadis (2019), the average processing time to reach the target concentration is 0.4 h larger if using a single scenario with MPC with thermal stability criterion $\mathcal{K}$. In Kähm and Vassiliadis (2018b) it is further shown that constant temperature MPC results in processing times of approximately 13 h. Hence, even with 10 scenarios and criterion $\mathcal{K}$, a 2-fold reduction in processing time can be achieved. Therefore, the conservative nature of scenario-based MPC does not hinder the ability to intensify processes.

Similar results are observed when embedding Lyapunov exponents within the scenario-based MPC framework. The processing times using Lyapunov exponents are shorter than those with criterion $\mathcal{K}$. Furthermore, as the number of scenarios employed increases, the control scheme becomes more conservative hence resulting in longer processing times.

Interesting to note is the apparent reduction in processing time when using Lyapunov exponents with up to 3 scenarios, as opposed to the nominal case shown in Figure 18: in the deterministic case there will always be the same extent of conservativeness which leads to a certain batch duration. When sampling different values for the set of uncertain parameters, it is possible to obtain a set of model parameters less likely resulting in thermal runaway behaviour. Hence less conservative process control can be achieved with even up 3 scenarios, as shown in Figure 21. Once more scenarios are used, it now becomes less and less likely to obtain a set of model parameters which predict the system to be less exothermic than it actually is. Therefore the batch duration starts to exceed that of the nominal case.

The increase in computational time due to the increased number of scenarios used for MPC is extremely important for this case study, as an industrial process is considered. The average computational times per MPC step obtained using scenario-based MPC are shown in Figure 22.

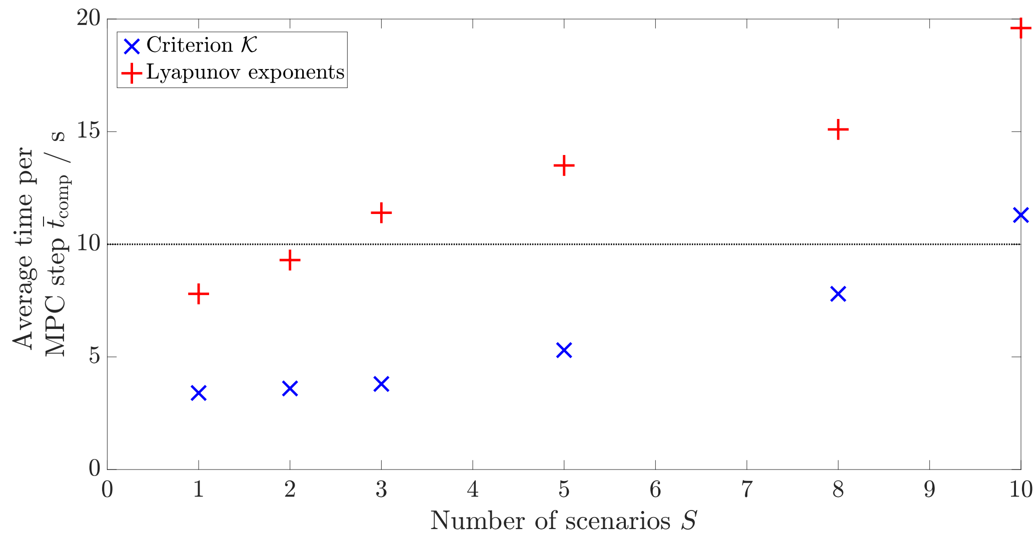

Figure 22: Computational times $\bar{t}_{\mathrm{comp}}$ per MPC step for the nitration of toluene with each number of scenarios. The horizontal dashed line indicates the upper limit of the computational time available for the MPC framework used.

With criterion $\mathcal{K}$, for 1 to 3 scenarios used the computational time is approximately 4 s. If more than 5 scenarios are used the computational time increases significantly. This feature is most likely observed due to 4 cores being available for each simulation. As the number of scenarios used exceeds 4, significant lag times are present for the evaluation of the additional scenarios. If up to 4 scenarios are present, the increase in computational time is most likely caused by an increase in communication time between the cores for the overall MPC algorithm. Using up to 5 scenarios results in an MPC framework which leaves enough time for data processing.

When using Lyapunov exponents a more significant increase in computational time per MPC step is observed. Therefore, if using more than 2 scenarios, the 10 s limit given by the MPC algorithm is exceeded. If larger systems were to be controlled with scenario-based MPC embedded with Lyapunov exponents, an even larger number of exponents would be required, further increasing the computational time. Hence, significant speed-up of the MPC framework with Lyapunov exponents is required for potential application in industry with the scenario-based approach.

5.2. Worst case MPC

In the introduction the *worst case* approach was briefly introduced. For the processes considered in this work it can easily be observed how a change in the identified parameters leads to higher potential

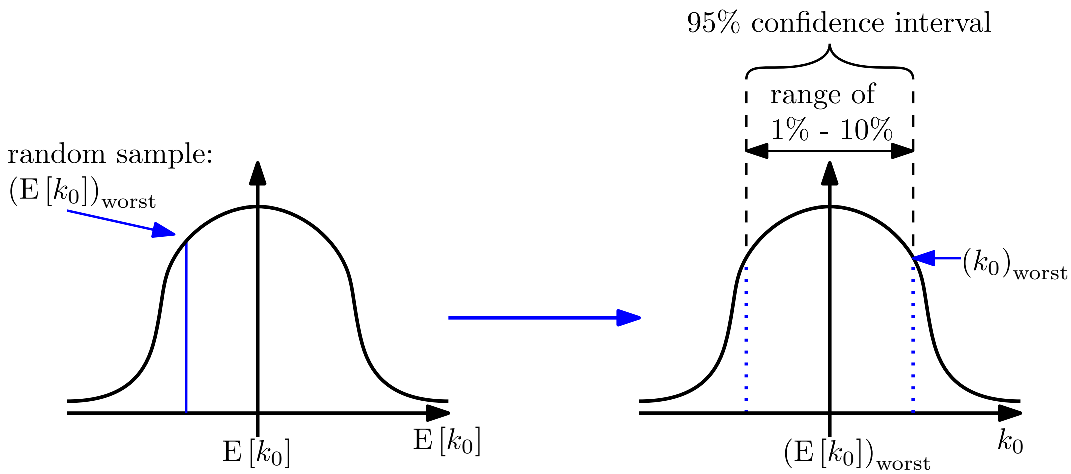

Figure 23: Schematic showing the sampling procedure to obtain the worst value of k_0 for the worst case MPC algorithm.

of thermal runaway behaviour:

- increase in $\Delta H_r \rightarrow$ increased heat generation
- increase in $k_0 \rightarrow$ faster reaction rate $\rightarrow$ increased heat generation
- decrease in $E_a \rightarrow$ faster reaction rate $\rightarrow$ increased heat generation
- decrease in $U \rightarrow$ decreased rate of heat removal

Therefore, given a range of values each parameter is allowed to take, the worst set of parameters can be found easily. Since process stability is of utmost importance the worst case MPC method will be used also.

Similarly to the scenario-based MPC analysis the nitration of toluene is considered below. MPC embedded with criterion $\mathcal{K}$ and with Lyapunov exponents are both used. The performance of each control scheme is compared in terms of number of processes causing thermal runaways, processing time and computational time per MPC step.

Unlike the analysis for scenario-based MPC, the mean values of each uncertain parameter are sampled using the distributions similar to those shown in Table 4. The key difference is the range in values chosen to be the 95% confidence interval: in Table 4 it was assumed that a range of 5% RSD is within the 95% confidence interval. The worst case is chosen to be at the boundary of this confidence interval, but the deviation from the mean is varied. Hence, the 95% confidence interval is used for a deviations of 1%, 3%, 5%, 8% and 10% of the mean value. This procedure is schematically shown for the Arrhenius pre-exponential factor k_0 in Figure 23.

Consider process P_5, for which the mean and standard deviation of k_0 are shown in Table 4. For a deviation of 8% from the mean the following worst case value would be used:

$$k_0 \sim \mathcal{N}\left(\mu_{k_0},\, \sigma_{k_0}^2\right) \tag{22a}$$

$$k_0 \sim \mathcal{N}\left(3.00 \times 10^5,\, 5.85 \times 10^7\right) \tag{22b}$$

A random sample from the above distribution yields:

$$(\mu_{k_0})_{\text{worst}} = 2.60 \times 10^5 \tag{23}$$

The worst case scenario mean, $(\mu_{k_0})_{\text{worst}}$, is used to find the standard deviation of the new distribution, including the required 8% deviation from the mean which sets the 95% confidence interval:

$$\sigma_{\text{worst}} = \frac{(\mu_{k_0})_{\text{worst}}}{1.96} \times 0.08 \tag{24a}$$

$$\sigma_{\text{worst}} = 1.06 \times 10^4 \tag{24b}$$

An increase in the Arrhenius pre-exponential factor will result in a faster reaction. Hence, the worst case value for k_0 from the new distribution, whilst staying within the 95% confidence interval, is given by:

$$(k_0)_{\text{worst}} = (\mu_{k_0})_{\text{worst}} + \sigma_{\text{worst}} \tag{25a}$$

$$(k_0)_{\text{worst}} = 2.60 \times 10^5 + 1.06 \times 10^4 \tag{25b}$$

$$(k_0)_{\text{worst}} = 2.71 \times 10^5 \tag{25c}$$

The same procedure is carried out for all remaining parameters. It is expected that as the deviation from the mean values increases, the resulting control system becomes more conservative. As the processes become more conservative the number of thermal runaway reactions decreases, and processing times increase.

100 simulations are carried out for the nitration of toluene with the worst case MPC approach embedded with criterion $\mathcal{K}$ and Lyapunov exponents. The fraction of processes resulting in thermal runaway behaviour is shown in Figure 24.

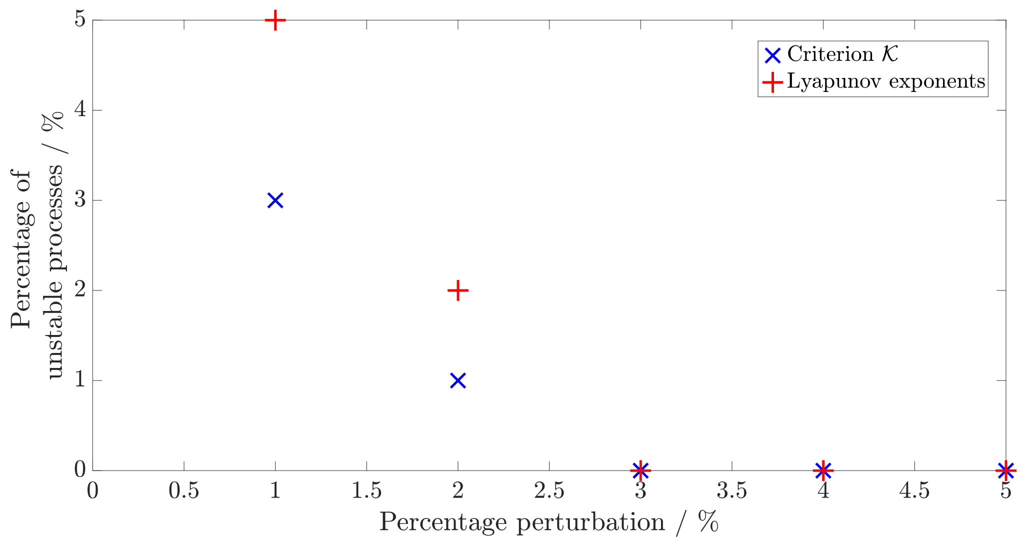

Figure 24: Fraction of simulations for the nitration of toluene resulting in thermal runaway behaviour for each percentage perturbation resulting in the worst case model.

In Figure 24 it is seen that an increase in the change of parameter values results in fewer thermal runaway processes. This is the case because the parameters obtained with a larger perturbation in their respective values results in a model with higher thermal runaway potential. As the potential of thermal runaway of the model used increases, the likelihood of keeping the nominal process under control increases. For a 3% change in the parameter values no thermal runaway behaviour is observed for the simulations carried out with both criterion $\mathcal{K}$ and Lyapunov exponents. The effect of increasing the thermal runaway potential of the model used on the processing time is shown in Figure 25.

As the percentage change in parameter values increases, a higher processing time t_{reac} is required to reach the target concentration. This is as expected, because an overall more conservative control scheme is obtained as the percentage change in parameter values increases. Important to note is the longer processing time when using criterion $\mathcal{K}$ with worst case MPC. For each set of simulations it is found that approximately 1 h more is required when stability criterion $\mathcal{K}$ is used instead of Lyapunov exponents. How the two different MPC schemes compare in terms of computational time required per MPC step, $\bar{t}_{\mathrm{comp}}$, is shown in Figure 26.

As the percentage change in parameter values increases, still a single scenario is simulated to evaluate each stability criterion. Hence no increase in computational time is observed. Due to the computational cost of evaluating Lyapunov exponents for each reagent and the reactor temperature, the computational cost per MPC step when using Lyapunov exponents is approximately double that of using criterion $\mathcal{K}$ with MPC. Using worst case MPC with Lyapunov exponents is close to the upper limit of 10 s available for each MPC iteration. Therefore significant speed-up of this control scheme

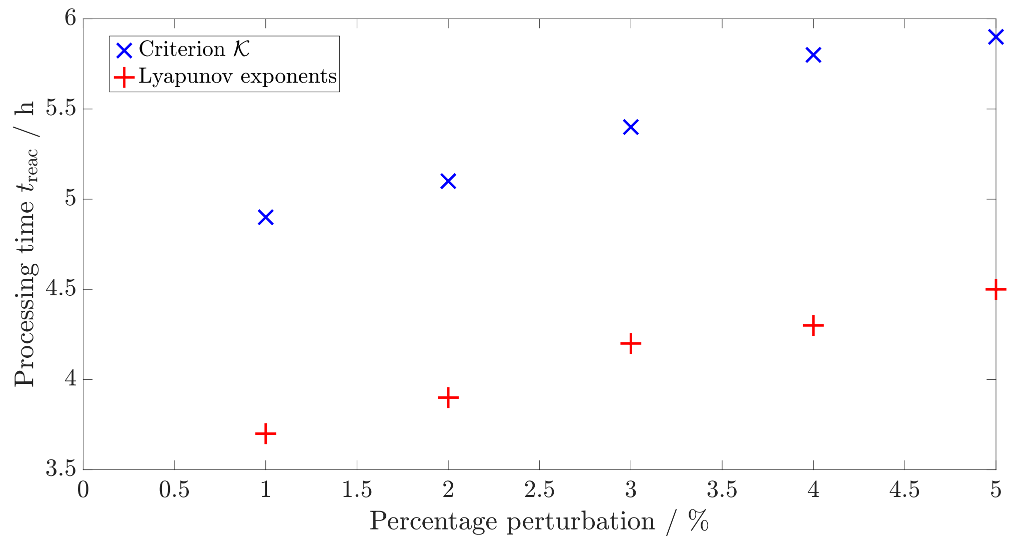

Figure 25: Processing times t_{reac} to reach the target concentration of o-nitrotoluene for the nitration of toluene for each percentage perturbation resulting in the worst case model.

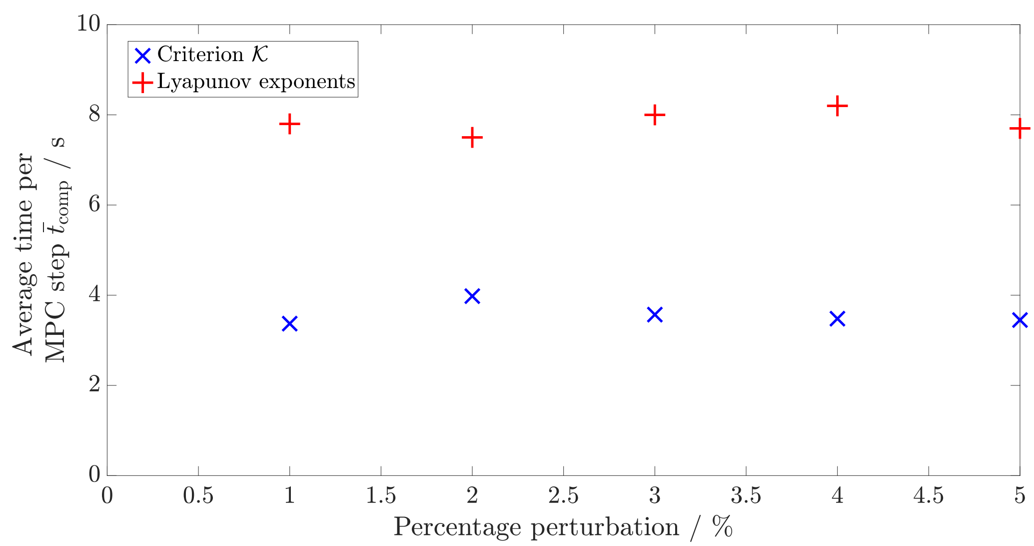

Figure 26: Computational times $\bar{t}_{\mathrm{comp}}$ per MPC step for the nitration of toluene for each percentage perturbation resulting in the worst case model.

would be required for industrial implementation. The MPC framework using worst case scenarios and criterion $\mathcal{K}$ on the other hand takes approximately 4 s per MPC step and therefore enough time for data processing at each MPC iteration is available.

6. Conclusions and further work

The goal of this work was the development of robust MPC frameworks for the safe intensification of batch processes using thermal stability criteria.

It is shown that stability criteria for systems with a clearly defined steady-state operating point, commonly found in literature, cannot be applied to batch processes. Such criteria include the Semënov criterion and the Routh-Hurwitz criterion. Therefore thermal stability criterion $\mathcal{K}$ and Lyapunov exponents, shown in literature to work for batch processes, are used as the basis for the robust MPC frameworks developed.

Parametric uncertainty is identified as the main source of uncertainty, assuming the model structure is accurate. The effect of uncertainty in most system parameters are examined, and 4 key parameters are identified: the enthalpy of reaction, the Arrhenius pre-exponential factor, the activation energy, and the heat transfer coefficient. Since an Arrhenius rate expression is used to describe the reaction rates, the uncertainty in the activation energy will have the largest effect on the thermal stability prediction. Assuming normal distributions for each parameter value, a 1% RSD is used for the activation energy and 5% RSD for the remaining 3 parameters is assumed. With these values robust MPC frameworks are examined.

Scenario-based MPC and worst case MPC are used for the purpose of robust MPC. The normal distributions for each parameter outlined above are applied to each MPC framework. The nitration of toluene is used as the case study for the purpose of comparing each robust MPC framework. It is found that each MPC framework results in safe processes, whilst intensifying the reaction by increasing the reactor temperature throughout.

As the number of scenarios used for scenario-based MPC, the computational time required per MPC step increases significantly. Since an upper limit of 10 s is present within the MPC algorithm, only a limited number of scenarios can be used. Worst case MPC, on the other hand, does not suffer from this issue: to achieve more conservative operation the worst set of parameters can be changed, whilst still requiring a single scenario to be simulated. Therefore the same extent of stability and process intensification as for scenario-based MPC can be achieved without a considerable increase in computational time. This can be done for the processes considered in this work, because it is obvious what set of values for the uncertain parameters results in higher thermal runaway potential.

Future work includes an analysis of a combination of the two approaches used here: multiple worst case scenarios. Such an approach can potentially result in reduced computational times whilst reducing the number of unstable processes. Additionally the assessment of the effect of model-plant mismatch with respect to model structure has to be investigated. Furthermore, the effect of measurement noise on the thermal stability prediction with criterion $\mathcal{K}$ and Lyapunov exponents is required for potential application in industry. In real plants state variables such as concentrations might not be directly measurable. Hence, estimation techniques such as Kalman filters are necessary to simulate how the robust MPC algorithm presented here would work in such a framework. Lastly, larger case studies have to be considered if such an MPC framework were to be applied in industry.

Acknowledgments

We thank the Engineering and Physical Sciences Research Council (EPSRC) and the Department of Chemical Engineering and Biotechnology, University of Cambridge, for funding the EPSRC PhD studentship for this project (DTP - University of Cambridge, Funder reference EP/M508007/1).

References

Albalawi, F., Alanqar, A., Durand, H., Christofides, P.D., 2016. A feedback control framework for safe and economically-optimal operation of nonlinear processes. American Institute of Chemical Engineers Journal 62, 2391–2409.

Albalawi, F., Durand, H., Christofides, P.D., 2017. Process operational safety using model predictive control based on a process Safeness Index. Computers & Chemical Engineering 104, 76–88.

Albalawi, F., Durand, H., Christofides, P.D., 2018. Process operational safety via model predictive control: Recent results and future research directions. Computers & Chemical Engineering 114, 171–190.

Anagnost, J.J., Desoer, C.A., 1991. An elementary proof of the Routh-Hurwitz stability criterion. Circuits Systems Signal Process 10.

Anucha, S., Chayavivatkul, V., Banjerdpongchai, D., 2015. Comparison of pid control and linear model predictive control application to regenerative thermal oxidizer system, in: Control Conference (ASCC).

Badwe, A., Patwadhan, R., Shah, S.L. an dPatwardhan, S., Gudi, R., 2010. Quantifying the impact of model-plant mismatch on controller performance. Journal of Process Control .

Baerns, M., Renken, A., 2004. Chemische Reaktionstechnik. Wiley-VCH. chapter 4.

Balakotaiah, V., 1989. Simple runaway criteria for cooled reactors. American Institute of Chemical Engineers Journal 35, 1039–1043.

Barkelew, C., 1959. Stability of chemical reactors. Chemical Engineering Progress Symposium Series 25, 37–46.

Bernadini, D., Bemporad, A., 2009. Scenario-based model predictive control of stochastic constrained linear systems, in: 48th IEEE Conference on Decision and Control, pp. 6333–6338.

Bosch, J., Strozzi, F., Zbilut, J., Zaldívar, J.M., 2004. On-line runaway detection in isoperibolic batch and semibatch reactors using the divergence criterion. Computers and Chemical Engineering 28, 527–544.

Bradford, E., Schweidtmann, A.M., Lapkin, A., 2018. Efficient multiobjective optimization employing Gaussian processes, spectral samplingand a genetic algorithm. Journal of Global Optimization 71, 407–438.

Campo, P.J., Morari, M., 1987. Robust model predictive control, in: Proceedings of the American control conference, pp. 1021–1026.

Cellier, F., Kofman, E., 2006. Continuous system simulation. Springer Science+Business Media.

Chatelin, F., 2012. Eigenvalues of Matrices. Society for Industrial and Applied Mathematics.

Chen, D., Seborg, D., 2003. Design of decentralized pi control systems based on nyquist stability analysis. Journal of Process Control 13, 27–39.

Chen, L.P., Chen, W.H., Liu, Y., Peng, J.H., Liu, R.H., 2008. Toluene mono-nitration in a semi-batch reactor. Central European Journal of Energetic Materials 5, 37–47.

Christofides, P.D., Liu, J., Muñoz de la Peña, D., 2011. Networked and Distributed Predictive Control. Springer, London. chapter 2. pp. 13–45.

Chuong La, H., Potschka, A., Bock, H.G., 2017. Partial stability for nonlinear model predictive control. Automatica 78, 14–19.

Davis, M., Davis, R., 2003. Fundamentals of Chemical Reaction Engineering. McGraw-Hill. chapter 2. pp. 53–56.

Dochain, D., 2003. State and parameter estimation in chemical and biochemical processes: a tutorial. Journal of Process Control 13, 801–818.

Frank-Kamenet͡skiĭ, D., 1969. Diffusion and Heat Transfer in Chemical Kinetics. Plenum Press.

Halder, R., Lawal, A., Damavarapu, R., 2008. Nitration of toluene in a microreactor. Catalysis Today 125, 74–80.

Hong, W., Lie, X., Zhihuan, S., 2012. A review for model plant mismatch measures in process monitoring. Chinese Journal of Chemical Engineering 20, 1039–1046.

Hurwitz, A., 1895. Über die Bedingungen, unter welchen eine Gleichung nur Wurzeln mit negativen reellen Theilen besitzt. Mathematische Annalen 46, 273–284.

James, G., Burley, D., Clements, D., Dyke, P., Searl, J., Wright, J., 2007. Modern Engineering Mathematics. Pearson Prentice Hall. chapter 5. Fourth edition. pp. 387–404.

Jones, D.R., Schonlau, M., Welch, W.J., 1998. Efficient global optimization of expensive black-box functions. Journal of Global Optimization 13, 455–492.

Joseph, E.A., Olaiya, O.O., 2018. Cohen-Coon PID Tuning Method: A Better Option to Ziegler Nichols-Pid Tuning Method. Computer Engineering and Intelligent Systems 9, 33–37.

Kähm, W., Vassiliadis, V.S., 2018a. Lyapunov exponents with model predictive control for exothermic batch reactors, in: IFAC-PapersOnLine.

Kähm, W., Vassiliadis, V.S., 2018b. Optimal laypunov exponent parameters for stability analysis of batch reactors with model predictive control. Computers and Chemical Engineering 119, 270–292.

Kähm, W., Vassiliadis, V.S., 2018c. Stability criterion for the intensification of batch processes with model predictive control. Chemical Engineering Research and Design 138, 292–313.

Kähm, W., Vassiliadis, V.S., 2018d. Thermal stability criterion integrated in model predictive control for batch reactors. Chemical Engineering Science 188, 192–207.

Kähm, W., Vassiliadis, V.S., 2019. Thermal stability criterion of complex reactions for batch processes. Chemical Engineering Research and Design ACCEPTED.

Kalmuk, A., Tyushev, K., Granichin, O., Yuchi, M., 2017. Online parameter estimation for MPC model uncertainties based on LSCR approach. 1st Annual IEEE Conference on Control Technology and Applications, CCTA 2017 , 1256–1261.

Kocijan, J., Murray-Smith, R., Rasmussen, C.E., Girard, A., 2004. Gaussian process model based predictive control, in: American Control Conference, 2004, pp. 2214—2219.

Likar, B., Kocijan, J., 2007. Predictive control of a gas-liquid separation plant based on a Gaussian process model. Computers & Chemical Engineering 31, 142—152.

Lucia, S., Andersson, J.A., Brandt, H., Bouaswaig, A., Diehl, M., Engell, S., 2014. Efficient Robust Economic Nonlinear Model Predictive Control of an Industrial Batch Reactor. IFAC Proceedings Volumes 47, 11093–11098.

Lucia, S., Finkler, T., Engell, S., 2013. Multi-stage nonlinear model predictive control applied to a semi-batch polymerization reactor under uncertainty. Journal of Process Control 23, 1306–1319.

Luo, K.M., Chang, J.G., 1998. The stability of toluene mononitration in reaction calorimeter reactor. Journal of Loss Prevention in the Process Industries 11, 81–87.

Maciejowski, J.M., Yang, X., 2013. Fault tolerant control using Gaussian processes and model predictive control, in: Conference on Control and Fault-Tolerant Systems (SysTol), IEEE, pp. 1–12.

Martí, R., Lucia, S., Sarabia, D., Paulen, R., Engell, S., de Prada, C., 2015. Improving scenario decomposition algorithms for robust nonlinear model predictive control. Computers and Chemical Engineering 79, 30–45.

Mawardi, M., 1982. The nitration of monoalkyl benzene and the separation of its isomers by gas chromatography. Pertanika 5, 7–11.

Mayne, D., Seron, M., Rakovic, S., 2005. Robust model predictive control of constrained linear systems with bounded disturbances. Automatica 41, 219–224.

Mayne, D.Q., 2014. Model predictive control: Recent developments and future promise. Automatica 50, 2967–2986.

Muñoz-Carpintero, D., Kouvaritakis, B., Cannon, M., 2016. Striped Parameterized Tube Model Predictive Control. Automatica 67, 303–309.

Rakovic, S., Kouvaritakis, B., Cannon, M., Panos, C., Findeisen, R., 2011. Fully parameterized tube MPC, in: Proceedings of the 18th IFAC World Congress, pp. 197–202.

Rasmussen, C.E., Williams, C.K.I., 2006. Gaussian Processes for Machine Learning. MIT Press. chapter 2.

Rawlings, J., Animit, R., 2009. Nonlinear model predictive control. Springer. chapter Optimizing process economic performance using model predictive control. pp. 119–138.

Rawlings, J., Mayne, D., 2015. Model Predictive Control: Theory and Design. Nob Hill Publishing. chapter 1. pp. 1–60.

Routh, E., 1877. A treatise on the stability of a given state of motion: Particularly steady motion. Macmillan .

Rupp, M., 2015. Über die Ethoxylierung von Octanol im Mikrostrukturreaktor. Ph.D. thesis. Universität Stuttgart, Fakultät für Energie-, Verfahrens- und Biotechnik.

Scokaert, P.O.M., Mayne, D.Q., 1998. Min-max feedback model predictive control for constrained linear systems. IEEE Transactions on Automatic Control 43, 1136–1142.

Semënov, N., 1940. Thermal theory of combustion and explosion, in: Progress of Physical Science (U.S.S.R).

Shampine, L., Reichelt, M., Kierzenka, J., 1999. Solving index-1 daes in matlab and simulink. SIAM Review 41, 538–552.

Sheats, G., Strachan, A., 1978. Rates and activation energies of nitronium ion formation and reaction in the nitration of toluene in 78% sulphuric acid. Canadian Journal of Chemistry 56, 1280–1283.

Sirohi, A., Choi, K.Y., 1996. On-Line Parameter Estimation in a Continuous Polymerization Process. Industrial and Engineering Chemistry Research 35, 1332–1343.

Stephanopoulos, G., 1984. Chemical Process Control. PTR Prentice Hall. chapter 14. pp. 258–279.

Strozzi, F., Zaldívar, J., 1999. On-line runaway detection in batch reactors using chaos theory techniques. American Institute of Chemical Engineers Journal 45, 2429–2443.

Theis, A., 2014. Case study: T2 Laboratories explosion. Journal of Loss Prevention in the Process Industries 30, 296–300.

Winde, M., 2009. Systematische Bewertung und Ertüchtigung von industriellen Regelkreisen in verfahrenstechnischen Komplexen. Ph.D. thesis. Ruhr-Universität Bochum, Fakultät für Maschinenbau.

Yucelen, T., Kaymakci, S., Kurtulan, S., 2006. Self-Tuning PID Controller Using Ziegler-Nichols Method for Programmable Logic Controllers.

Zhang, Z., Wu, Z., Durand, H., Albalawi, F., Christofides, P.D., 2018. On integration of feedback control and safety systems: Analyzing two chemical process applications. Chemical Engineering Research and Design 132, 616–626.